การศึกษาเชิงตัวเลขของการผสมของของไหลสองชนิดที่ไม่ละลายเข้าหากันในเครื่องปฏิกรณ์แบบจานหมุน

นายพิชญะ สมภพสกุล

วิทยานิพนธ์นี้เป็นส่วนหนึ่งของการศึกษาตามหลักสูตรปริญญาวิศวกรรมศาสตรมหาบัณฑิต
สาขาวิชาวิศวกรรมเครื่องกล ภาควิชาวิศวกรรมเครื่องกล
คณะวิศวกรรมศาสตร์ จุฬาลงกรณ์มหาวิทยาลัย
ปีการศึกษา 2559

NUMERICAL STUDY OF TWO IMMISCIBLE LIQUIDS MIXING IN A SPINNING DISC REACTOR

Mr. Pichaya Sompopskul

A Thesis Submitted in Partial Fulfillment of the Requirements
for the Degree of Master of Engineering Program in Mechanical Engineering
Department of Mechanical Engineering
Faculty of Engineering
Chulalongkorn University
Academic Year 2016

Thesis Title	NUMERICAL STUDY OF TWO IMMISCIBLE LIQUIDS MIXING IN A SPINNING DISC REACTOR
By	Mr. Pichaya Sompopskul
Field of Study	Mechanical Engineering
Thesis Advisor	Assistant Professor Sompong Putivisutisak, Ph.D.
Thesis Co-Advisor	Professor Suttichai Assabumrungrat, Ph.D.

Accepted by the Faculty of Engineering, Chulalongkorn University in Partial Fulfillment of the Requirements for the Master's Degree

.....Dean of the Faculty of Engineering
(Associate Professor Supot Teachavorasinskun, Ph.D.)

THESIS COMMITTEE

.....Chairman
(Associate Professor Boonchai Lertnuwat, Ph.D.)
.....Thesis Advisor
(Assistant Professor Sompong Putivisutisak, Ph.D.)
.....Thesis Co-Advisor
(Professor Suttichai Assabumrungrat, Ph.D.)
.....External Examiner
(Weerinda Appamana, D.Eng.)

พิชญะ สมภพสกุล : การศึกษาเชิงตัวเลขของการผสมของของไหลสองชนิดที่ไม่ละลายเข้าหากันในเครื่องปฏิกรณ์แบบจานหมุน (NUMERICAL STUDY OF TWO IMMISCIBLE LIQUIDS MIXING IN A SPINNING DISC REACTOR) อ.ที่ปรึกษาวิทยานิพนธ์หลัก: ผศ. ดร. สมพงษ์ พุทธิวิสุทธิศักดิ์, อ.ที่ปรึกษาวิทยานิพนธ์ร่วม: ศ. ดร. สุทธิชัย อัสสะบำรุงรัตน์ , 55 หน้า.

งานวิจัยนี้เป็นการศึกษาเชิงตัวเลขของการผสมของไหลสองชนิดที่ไม่ละลายเข้าหากันในเครื่องปฏิกรณ์แบบจานหมุน (spinning disc reactor, SDR) ซึ่งเครื่องปฏิกรณ์นี้ พบข้อได้เปรียบของที่ดีกว่าเครื่องปฏิกรณ์อื่น ๆ ทั่วไปจากงานวิจัยที่ผ่านมา การจำลองการผสมภายในเครื่องปฏิกรณ์แบบจานหมุนนี้ใช้โปรแกรมสำเร็จรูป ANSYS Fluent 15.0.7 ซึ่งใช้ระเบียบวิธีไฟไนต์วอลุมในการแปลงสมการอนุรักษ์มวลและโมเมนตัม รวมถึงสมการระเบียบวิธี VOF เป็นสมการพีชคณิต และการประมาณค่าตัวแปรใช้ขั้นตอนวิธี QUICK และ Compressive สำหรับรูปแบบเครื่องปฏิกรณ์แบบจานหมุนที่ใช้ในงานวิจัยนี้จะป้อนของเหลวที่ไม่ละลายเข้าหากันจากทางด้านบน ได้แก่น้ำและนอร์มอลเฮปเทน แล้วคำนวณพื้นที่ผิวสัมผัสระหว่างสองสารและเวลาที่สารอยู่ในเครื่องปฏิกรณ์ อัตราเร็วการหมุนของจานถูกปรับตั้งแต่ 10 จนถึง 2500 รอบต่อนาที และอัตราการไหลของแต่ละของเหลวตั้งแต่ 5.330 จนถึง 15.708 มิลลิลิตรต่อวินาที หลังจากที่คำนวณทุกกรณีแล้ว พบว่าช่วงของอัตราเร็วการหมุนที่เหมาะสมคือ 50 ถึง 250 รอบต่อนาที ถ้าอัตราเร็วเลยจากช่วงนี้ไปจะทำให้ฟิล์มของเหลวผสมที่อยู่บนจานไม่เสถียร ช่วงของพื้นที่ผิวสัมผัสที่คำนวณได้อยู่ระหว่าง 4.97×10^{-3} ถึง 6.35×10^{-2} ตารางเมตร และช่วงของเวลาที่อยู่ในเครื่องปฏิกรณ์คือ 0.5 ถึง 3.4 วินาที พื้นที่ผิวสัมผัสระหว่างของเหลวจะเพิ่มขึ้นเมื่อเพิ่มอัตราการไหล แต่ลดลงเมื่อเพิ่มอัตราเร็วการหมุน เวลาที่อยู่ในเครื่องปฏิกรณ์ของน้ำและนอร์มอลเฮปเทนจะลดลงเมื่อเพิ่มอัตราการไหลหรือเพิ่มอัตราเร็วการหมุน ยิ่งกว่านั้น อัตราเร็วที่สูงจะทำให้ความหนาของฟิล์มของเหลวสม่ำเสมอ การเพิ่มจำนวนหัวจ่ายของเหลวหรือขยับหัวจ่ายออกห่างจากศูนย์กลางแบบเท่า ๆ กันทำให้พื้นที่ผิวสัมผัสระหว่างของเหลวลดลง แต่ว่าการวางตำแหน่งหัวจ่ายที่ไม่สมมาตรมีความเป็นไปได้ที่จะเพิ่มพื้นที่ผิวสัมผัส ดังนั้นการออกแบบเพื่อปรับปรุงสมรรถนะของเครื่องปฏิกรณ์แบบจานหมุน ตอนนี้ยังมีความหลากหลายอยู่และรอการค้นคว้าเพิ่มเติม เช่น การปรับและจัดวางตำแหน่งของหัวจ่าย ความขรุขระของแผ่นจานหมุน และลักษณะตัวเรือน (casing) ของเครื่องปฏิกรณ์ เป็นต้น

ภาควิชา	วิศวกรรมเครื่องกล	ลายมือชื่อนิสิต .....
สาขาวิชา	วิศวกรรมเครื่องกล	ลายมือชื่อ อ.ที่ปรึกษาหลัก .....
ปีการศึกษา	2559	ลายมือชื่อ อ.ที่ปรึกษาร่วม .....

5770249521 : MAJOR MECHANICAL ENGINEERING
KEYWORDS: SPINNING DISC REACTOR / MULTIPHASE FLOW / IMMISCIBLE LIQUID / THIN FILM

PICHAYA SOMPOPSKUL: NUMERICAL STUDY OF TWO IMMISCIBLE LIQUIDS MIXING IN A SPINNING DISC REACTOR. ADVISOR: ASST. PROF. SOMPONG PUTIVISUTISAK, Ph.D., CO-ADVISOR: PROF. SUTTICHAI ASSABUMRUNGRAT, Ph.D., 55 pp.

A numerical study of mixing two immiscible liquids in the spinning disc reactor (SDR) is performed with a commercial CFD software, ANSYS Fluent 15.0.7. Many advantages of the SDR over conventional reactors were reported in literatures. For the simulation of the mixing flow inside this reactor. General conservation equations and VOF method are taken into account and discretized by a finite volume method. The QUICK and Compressive schemes are used for interpolation of interfacial variables. The SDR studied in this work has two inlets at the top which feed different immiscible liquids. Water and n-heptane were selected for the computation of interfacial area between phases and its mean residence time in the reactor, which lead to mixing and product yielding performance. The rotating speeds of 10 to 2500 rpm and the liquid flow rate of 5.330 to 15.708 mL/s each are varied. After all cases were computed, the appropriate range of rotating speed is found to be 50 to 250 rpm. Beyond the range, the liquid film inside the SDR faces the instability of film itself. The range of the computed interfacial area and the residence time are between 4.97×10^{-3} to 6.35×10^{-2} m^2 and 0.5 to 3.4 seconds, respectively. The interfacial area is found to increase with the liquid flow rate but not the rotating speed. The residence times of water and n-heptane decrease when the flow rate or rotating speed increases. Moreover, the high rotating speed seems to have an ability to maintain the uniform distribution of the liquid film. Adding two more liquid inlets or equally shifting inlets from the center reduces the interfacial area. However, arranging the inlets asymmetrically has a potential to increase the interfacial area. Therefore, there are still having various choices of design to be discovered, such as feeding inlet configuration, disc surface roughness and stationary casing, for the improvement of the reactor performance in the future.

Department:	Mechanical Engineering	Student's Signature	.....
Field of Study:	Mechanical Engineering	Advisor's Signature	.....
Academic Year:	2016	Co-Advisor's Signature	.....

ACKNOWLEDGEMENTS

I would like to acknowledge the support from Ratchadapiseksomphot Endowment under Outstanding Research Performance Program and the Thailand Research Fund (DPG5880003).

CONTENTS

Page

LIST OF FIGURES

LIST OF TABLES

NOMENCLATURES

VARIABLES

A	interfacial area
$\vec{A}$	arbitrary vector
a	coefficient of algebraic equation
$\vec{a}$	absolute acceleration
b	algebraic source term
Δc	species concentration difference
D	diffusion conductance
F	convective mass flux per unit area
$\vec{f}$	force per volume
$\vec{g}$	gravitational acceleration
h	heat transfer coefficient
k	mass transfer coefficient
$\dot{n}$	rate of mass transfer
p	pressure
$\dot{q}$	heat rate
$\vec{r}$	position vector
S	source term
$\vec{S}$	surface vector
t	time variable
ΔT	temperature difference
$\vec{u}$	absolute velocity
V	volume
$\vec{V}$	relative velocity
X	volume fraction
β	slope limiter

δ	film thickness
δx	cell dimension
μ	dynamic viscosity
ρ	density
σ	area magnitude of a half volume fraction surface
ϕ	general property of fluid
Γ	diffusivity of any property
Ω	rotating speed
∇	del operator

SUPERSCRIPTS

T	matrix transpose
$'$	correction
$*$	guessed

SUBSCRIPTS

a	air
B	bottom point
E	east point
EE	two-step east point
ext	external
h	n-heptane
i	any one phase
m	mean residence time
nb	neighboring point
o	frame of reference origin
P	interested point
PE	from interested point to east
L	liquid
N	north point

S	south point
T	top point
W	west point
WP	from west to interested point
WW	two-step west point

ABBREVATIONS

CFD	computational fluid dynamics
SDR	spinning disc reactor

CHAPTER 1
INTRODUCTION

1.1 MOTIVATION

Now, we cannot refuse that we are living in the world of innovation. All the products are produced for satisfying endless demands of the mankind and developed for surviving in highly competitive markets. So, for every production, the industrial sector takes a very important role. To reduce costs, human labors were replaced by machines which can generate massive amount of products with less defects. The aforementioned form of production is called ‘mass production’. Food, medicine and chemical are some examples of the ‘mass products’, which is a class of products from mass production. However, many of mass products in daily life such as food seasoning, sauce, salad dressing, shampoo, liquid detergent and etc. have to undergo a mixing process or a chemical process for being done, and these processes need an equipment called ‘chemical reactor’ to achieve.

Chemical reactors are the main apparatus for industrial productions which implicate with the chemical process. Chemical reactions between reactant materials take place in a chemical reactor and form the products. Thus, for inducing more reaction rate and product uniformity, the reactions normally have to lean on a mixing process. There are many kinds of chemical reactor such as static mixers, rotating packed beds, microchannels and etc. [1, 2] Nevertheless, the conventional reactors that are still used in the factory often face production problems, for examples, difficulty of reparation and maintenance, taking a long residence time, discontinuity of operation and only usable for batch production constraint. However, a part of researches are keeping eyes on a type of reactor which might be a key for industrial mass production. Since, it has a simple structure, gives a high productivity, form a good mixing and, prominently, can operate continuously [1]. This reactor is called ‘spinning disc reactor’ or ‘SDR’.

But somehow, the researches about the spinning disc reactors are not much existing now. For this reason, that means, the SDR has a potential to be developed for increasing itself efficiency. Thus, there should be an investigation for beforehand understanding its behavior. To collect details and study in various cases as many as

possible, the numerical method, called CFD, is suitably chosen for this study. Many former researches confirmed the abilities of SDR above other reactors, but the SDR still have to improve its performance and efficiency for producing products at better quality and higher quantity. To be concretely indicated, mixing will be a representative of product both quality and quantity. To primarily determine mixing in an SDR, two different immiscible liquids are used for a clear observation of the mixing.

Therefore, this research then emphasizes on the study of the SDR performance and other related parameters. Mainly, the rotating speed is going to be observed its effects on the mixing and a product yield.

1.2 OBJECTIVES

1. To study the effect of disc rotating speed and other parameters on the spinning disc reactor performance e.g. residence time and contacting surface (interfacial area) between phases
2. Analyze the fluid dynamics of the flow, process and phenomena in a spinning disc reactor
3. Recommend operation guidelines for SDR to increase an efficiency of SDR operation.

1.3 SCOPES OF RESEARCH

1. Commercial ANSYS Fluent 15.0.7 was used for the simulation
2. The three-dimensional domain of SDR modelled in this research has two to four inlets at the top and the mixed fluid exit radially at the edge of disc
3. The process in the SDR is mixing of two immiscible liquids without reaction and mass transfer between phases

1.4 EXPECTED BENEFITS

After this research has been completed, it would make readers understand the details of phenomena occurring within an SDR more clearly and the effects of related variables. The data provided in the research would be a good fundamental for design,

improvement, development and optimization of SDR afterward for increasing efficiency of industrial production.

CHAPTER 2
LITERATURE REVIEW

After understanding the importance of studying an SDR in the first chapter, published researches about SDR have to be reviewed before going to the next step of this work. The general features, advantages and applications of SDR and its performance will be reviewed in this chapter, also some interesting results, comments and discussions from the former researchers.

2.1 SPINNING/ROTATING DISC REACTOR

A spinning (or rotating) disc reactor, abbreviated as SDR (or RDR respectively), is a continuously operated reactor [3]. It is composed of a rotating disc contained within a bordering stationary cylindrical case in general [1]. Input fluid flows can be fed into the reactor in many ways depend on various applications, also withdrawal of output flows. Mixing, and a chemical reaction if exists, of the inputs is normally performed in the regions nearby the disc surfaces which rotate during an operation. And when the disc is rotating, it creates a centrifugal field which radially casts the processed fluid against the rotating disc surface outward to the edge of the disc in a form of film flow.

Apart from the general described above, they are different features of each SDR, which design concepts are not clearly explained. For examples, flow inlet locations, they are placed above the center of rotating disc in the works of Chen and Chen [1], De Caprariis et al. [3] and Akhtar et al. [4] (Figure 2.1a, b and c, respectively), which mixing occurs on the upper side of the disc surface. But Visscher et al. [2] used the SDR with one inlet above near the disc center and another beneath the disc edge, as shown in Figure 2.1d. They cause the mixing occurs under the disc. That means, material feeding points of the reactor are not generally prescribed, but can have various configuration designs of the feeding points.

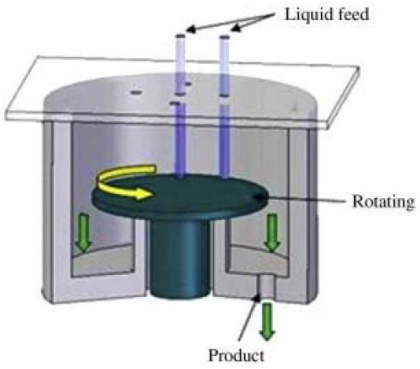

(a) De Caprariis et al. [3]

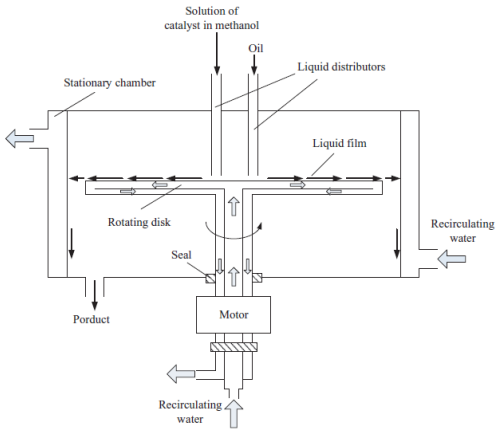

(b) Chen and Chen [1]

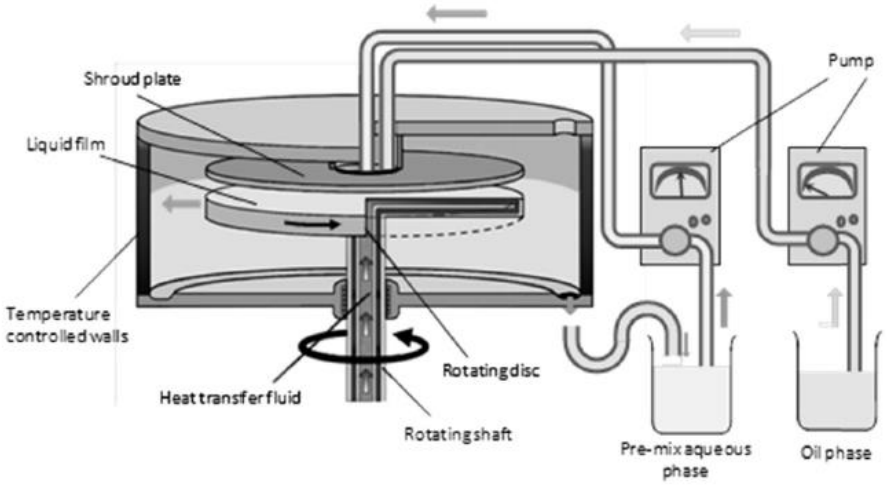

(c) Akhtar et al. [4]

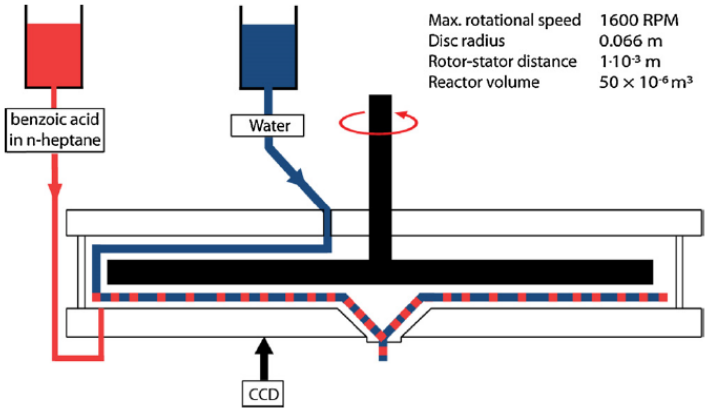

(d) Visscher et al. [2]

Figure 2.1 Spinning disc reactors from old works

Also the casings, some are wide and high, and the mixing flows freely on the disc [1, 3]. On the other hand, some have a stator, nearly placed in front of the disc surface which the mixing occurs, in the form of a shroud plate [4] or a flat casing [2]. It confines mixing in a limited space.

Many researchers who studied about the SDRs found the strengths and some advantages above the conventional reactors. Continuous operation and high mixing efficiency are what they had the same agreement and make the SDR be an appropriate choice for industrial applications [1]. Likewise, some researchers uniquely found their advantages of the SDR. Chen and Chen [1] found that an SDR reached the highest mixing efficiency above a continuous flow stirring reactor, a Couette flow reactor, a static mixer, an ultrasound-assisted flow cell and a rotating packed bed. Akhtar et al. [4] could run the mechanical and thermal process simultaneously in a single process, which gives an ease of controlling product quality and less energy consumption in the SDR-processed mayonnaise production. Visscher et al. [2] claimed that the SDR gave higher liquid mass transfer rates, from their case, compared to packed columns and microchannels. From the continuous nanoparticles production of De Caprariis et al. [3], the SDR was found having short residence time, which confined particle size distribution at the target size, and consumed less energy for mixing. Also they stated, an SDR is appropriate to reactions which essentially relies on mixing. Chen and Chen [1] used an SDR for producing biodiesel and got a high product yield and a small residence time, which they brought a high production rate. Furthermore, an SDR has a simple structure, maintenance ease and low cost, they informed. Akhtar et al. [4] confirmed that benefits of SDR are reduction of reaction time and residence time, mixing improvement and simple process.

From the general operation and advantages mentioned above, the SDRs can be used for many applications, such as mixing process, transesterification, precipitation, deposition and polymerization. And from the abilities to be continuously operated and very short residence time taken, the SDRs are very capable to be applied with industrial productions [1, 3, 5].

2.2 PERFORMANCE OF SPINNING DISC REACTOR

The performance of SDR changes with operating conditions. The main characteristic of SDR is the rotating speed which directly or indirectly affects other performances consequently, such as centrifugal force, shear force, mixing, turbulence, flow pattern, mass transfer rate of the contents, characteristics of the product and etc. Well-settled parameters will lead to high product yields.

Former researches stated some interesting relations of the operative parameters. Many of them told about the effect of rotating speed, but they looked at the different affected parameter. De Caprariis et al. [3] found that if the disc rotates fast will cause strong centrifugal field and intensify mixing. Specifically, in emulsification process, Akhtar et al. [4] minimized the mean droplet size of emulsion. Rotating speed also intensifies mass transfer [6] and reduces liquid film thickness on the disc surface [4]. Peshev et al. [6] additionally found that decreasing of rheology index of liquid can strengthen the effect of rotating speed.

Besides, disc rotation usually causes a velocity gradient, indicator of shear force occurrence in viscous fluids, which brings some consequences of performance changing. Achieving high liquid mass transfer rates is one of the consequences, from the study of Visscher et al. [2], and also attaining intensive mixing as De Caprariis et al. [3] found. Centrifugal force has a significant role to generate thin and highly sheared films on the disc surface in the study of isomerization process by Vicevic et al. [2], and also increase yield in the study of biodiesel production by Chen and Chen [1]. Qualitatively, different flow patterns could also create different product characteristics [5] and strongly affect liquid mass transfer rate [2]. A summary of performance relations from the literatures about SDR is illustrated in Figure 2.2.

In addition, the locations of raw material feeding points and product venting point are also now having the diversity of positioning. They could affect some performance of the reactor. For an example, in the nano-particles production process, a particle size distribution of the product depends on the feeding point location of reactants [2, 3, 5].

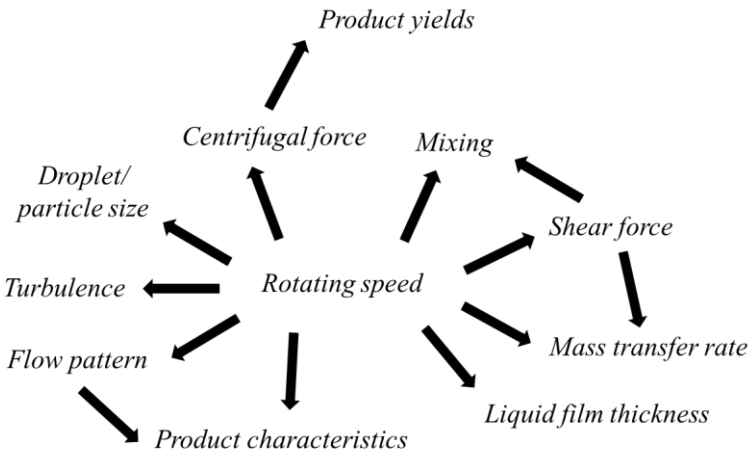

Figure 2.2 Summary of reviewed performance relations of SDR

2.3 OVERVIEW OF STUDY METHODOLOGIES

As SDR can be studied in many ways. Each literatures has its own method and aspect of the study. The summary of reviewed papers is shown in Table 2.1. Much of the works were not studied analytically, only the gypsum dissolution study by Peshev et al. [6] was done. A correlation to evaluate average mass transfer rates was derived, however, the mathematical model had been simplified intermediately before reached the final bulky expression. In many application of SDR, there are various ways how to operate the reactor, which cause the flow behavior inside be more complex and difficult to model in simple equations. That is why much of the studies about SDR were numerical and experimental.

As seen in the methodology summary, the parametric study is a popular aspect for the former researches. Perhaps, it is easy to explicate the works for the real applications, as they only focused on changing of inputs and yields. Nevertheless, the past parametric studies were not enough for direct implementation with disparate applications, because they were limited in a distinctive application and details inside the reactor were not revealed and understood.

Table 2.1 A summary of study methodologies from the literatures

Research work	Studying method	Work aspect
Continuous production of nanoparticles of HAP by wet chemical synthesis [3]	Numerical	Parametric study
Continuous alkaline-catalyzed transesterification of soybean oil and methanol [1]	Experimental	Optimization
Flow regimes in chemical vapor deposition [5]	Numerical	Parametric study
Extraction of benzoic acid from n-heptane to demineralized water [2]	Experimental	Parametric study
Dissolution of gypsum in two aqueous polymer solution [6]	Analytical	Mathematical model
Continuous process for making mayonnaise and salad cream [4]	Experimental	Application
Isomerization of α-pinene oxide to campholenic aldehyde [7]	Experimental	Parametric study

2.4 INTERESTING RESULTS FROM THE LITERATURES

Most of the reviewed papers have their own results which confirm the efficient performances of SDR above other conventional reactors. Chen and Chen [1] got the biodiesel yields of 96.9% from their research within a residence time of 2 to 3 seconds. Moreover, they got the biodiesel production rate of 1.86 mol/minutes which they claimed that it is higher than other continuous transesterification process reactor.

Visscher et al. [2] found the interesting effect of operating conditions to the overall mass transfer rates between two liquids. The mass transfer rate increased from 0.17 to 51.47 $m^3_{ORG}/m^3_R s$ when the rotating speed and water flow rate increased 16 and 5 times higher respectively. And this increased mass transfer rate was 25 times and 10-15 times higher when compared to packed columns and microchannels, respectively. Besides, qualitatively, they found the different flow patterns of the two liquids on each range of disc speeds. Below the disc speed of 100 rpm, the flow was in a continuous spiraling flow pattern. From 100 to 300 rpm, the flow was dispersed to small droplets

but still in a form of spiral. Finally, the flow was fully dispersed without noticeable spiraling structure.

In the nanoparticle production process of De Caprariis et al. [3], they found a similarity of velocity profiles between the profiles at the disc surface and the maximum liquid film height of 70 μm. And the concentration profile of the liquid product seemed to be congruent with the calculated reaction rate contour, which the highest values of reaction rates and production concentrations both located along the contact regions of reactants.

Another interesting results are from the research of Vicevic et al. [7], they got the best choice of catalysts used in the SDR-processed isomerization. The product selectivity of 75% and the reactant conversion of 85% were found at a disc temperature, rotating speed and reactant flow rate of 45 °C, 1500 rpm and 6 cm^3/s respectively.

2.5 SOME LITERATURE COMMENTS

Spinning disc reactors are now novel equipment for industrial productions. Some researchers suggested many interesting paths for the development of SDR in their discussions. Most of the papers studying about SDR emphasized on parametric study. However, the phenomena occurring inside are still questioned in details [5], that is why the SDR is now just a black box.

De Caprariis et al. [3] commented that an optimization of SDR is needed a clear explanation of fluid film dynamics on the disc, which has to be determined its turbulence for acceptable accuracy. Akhtar et al. [4] reminded, operating the reactor against high shear stress could make defects if the product is sensitive to a stress.

From the suggested comments above, the details of phenomena on the fluid dynamics aspect will be discussed later in this research, which includes velocity profiles and shear stresses of the flow. But this research will not delve into the turbulence behaviors of the mixing flow inside an SDR.

CHAPTER 3
RELATED THEORY AND NUMERICAL MODEL VALIDATION

After known about SDR in the previous chapter, the tool which will be applied to model an SDR have to be found. In this chapter, the phenomena that occur inside the SDR are going to be represented by mathematical models. And the numerical codes from the commercial simulation software, ANSYS Fluent 15.0.7, will be validated with fluid flows which partly have a related nature of the flow in a spinning disc reactor.

3.1 GOVERNING CONSERVATION EQUATIONS

To describe transport phenomena arising inside the SDR, while it is on operation, the conservation equations are needed for determining momentum transfer in the system. Continuity equation and momentum equation are stated below respectively in vector form.

$$\frac{\partial \rho}{\partial t} + \nabla \cdot (\rho \vec{u}) = 0 \tag{3.1}$$

$$\frac{\partial}{\partial t}(\rho \vec{u}) + \nabla \cdot (\rho \vec{u}\vec{u}) = -\nabla p + \nabla \cdot [\mu(\nabla \vec{u} + (\nabla \vec{u})^T)] + \rho \vec{g} + \vec{F}_{ext} \tag{3.2}$$

All the governing equations above have no exact solutions. Therefore, another method will take a role for solving this problem, which will be discussed in the chapter about the finite volume method.

3.2 MULTIPHASE MODELLING: VOLUME OF FLUID

The ordinary conservation equations are used for one-phase fluid flow. Since this research has to deal with a liquid flow more than one phase. The model for representing multiphase flow has to be proposed. The Volume of Fluid (VOF) [8] model is chosen, which can be written as

$$\frac{\partial}{\partial t}(X_i \rho_i) + \nabla \cdot (X_i \rho_i \vec{u}_i) = S_{X_i} \tag{3.3}$$

and the summation of volume fraction of all phases is equal to unity for any differential volumes in the space,

$$\sum_i X_i = 1 \tag{3.4}$$

where $0 \leq X_i \leq 1$.

For a computation of flow with n phases, the n-1 VOF equations are solved for volume fractions, except the primary phase which its volume fraction is calculated from Eq. 3.4 as a residual from other phases. However, the VOF equations are partial differential equations, same as the conservation equations. Therefore, a method of discretization for approximate the solutions will be explain in the next section.

3.3 FINITE VOLUME METHOD

As the governing partial differential equations cannot be solved analytically, there must be a method for estimating the solution. Many differential conservation equations are often in this general form.

$$\frac{\partial}{\partial t}(\rho\phi) + \nabla \cdot (\rho\phi\vec{u}) = \nabla \cdot \left(\Gamma_\phi \nabla\phi\right) + S_\phi \tag{3.5}$$

Each differential volumes in the computation domain is replaced by very small volumes with a finite size. And fluxes of property through surfaces of the volume will be determined by volumetric integration.

$$\int \left[\frac{\partial}{\partial t}(\rho\phi) + \nabla \cdot (\rho\phi\vec{u})\right] dV = \int \left[\nabla \cdot \left(\Gamma_\phi \nabla\phi\right) + S_\phi\right] dV$$

From Stokes' theorem

$$\oint \nabla \cdot \vec{A}\, dV = \oint \vec{A} \cdot d\vec{S}\,,$$

then

$$\int \frac{\partial}{\partial t}(\rho\phi) dV + \oint (\rho\phi\vec{u}) \cdot d\vec{S} = \oint \left(\Gamma_\phi \nabla\phi\right) \cdot d\vec{S} + \int S_\phi dV$$

After integrating on the small finite volume with the closed surface, finally, the general governing equation will be discretized to a form of algebraic equation, which can be generally written as

$$a_P \phi_P = \sum_{nb} a_{nb} \phi_{nb} + b\,. \tag{3.6}$$

3.4 DISCRETIZATION SCHEMES AND SOLUTION ALGORITHMS

The behavior of fluid flow is described by non-linear partial differential equations. The non-linearity in the convective terms of equations will cause complexity and can make the algebraic approximation unrealizable. Hence, there are many spatial discretization schemes to deal with the non-linearity and help the calculation of approximate solution to converge and accurate.

In this research, the transported fluid property variables in momentum equations is interpolated from neighboring cells by the Quadratic Upstream Interpolation for Convective Kinetics (QUICK) scheme of Leonard [9]. This numerical scheme is a second-order accuracy scheme, stated by

$$a_P\phi_P = a_E\phi_E + a_W\phi_W + a_{EE}\phi_{EE} + a_{WW}\phi_{WW}\ , \tag{3.7}$$

where

$$F_e = (\rho u)_e$$

$$F_w = (\rho u)_w$$

$$D_e = \frac{\Gamma_e}{\delta x_{PE}}$$

$$D_w = \frac{\Gamma_w}{\delta x_{WP}}$$

$$a_E = D_e + \tfrac{3}{8}\alpha_e F_e - \tfrac{6}{8}(1-\alpha_e)F_e - \tfrac{1}{8}(1-\alpha_w)F_w$$

$$a_W = D_w + \tfrac{6}{8}\alpha_w F_w + \tfrac{1}{8}\alpha_e F_e + \tfrac{3}{8}(1-\alpha_w)F_w.$$

$$a_{EE} = \tfrac{1}{8}(1-\alpha_e)F_e$$

$$a_{WW} = -\tfrac{1}{8}\alpha_w F_w.$$

$$a_P = a_E + a_W + a_{EE} + a_{WW} + (F_e - F_w).$$

and $\alpha_w = 1$ for $F_w > 0$ and $\alpha_e = 1$ for $F_e > 0$

$\alpha_w = 0$ for $F_w < 0$ and $\alpha_e = 0$ for $F_e < 0$

Although, in general, second-order schemes reduce numerical diffusion errors and raise accuracy above first-order schemes, they are reciprocated acquirement of better accuracy with the solution instability. [10]

For VOF equations, the Compressive scheme [11] is used for interpolation of volume fraction variables, which stated by

$$\phi_f = \phi_d + \beta \nabla \phi_d \, ,$$

Even though all partial differential equations are discretized to algebraic equations, velocity and pressure are still coupled in the equations. To solve the set of equations, Semi-Implicit Method for Pressure-Linked Equations or SIMPLE algorithm [12] is applied here. New variables are proposed, variable correction (ϕ') and guessed variable (ϕ^*), which can be either pressure (p) or velocity in each directions (u, v, w). The continuity equation is derived, using the new variables, as the pressure-correction equation

$$a_P p'_P = a_E p'_E + a_W p'_W + a_N p'_N + a_S p'_S + a_T p'_T + a_B p'_B + b \, , \tag{3.8}$$

where

$$a_E = \rho_e d_e \Delta y \Delta z \, ,$$

$$a_W = \rho_w d_w \Delta y \Delta z \, ,$$

$$a_N = \rho_n d_n \Delta x \Delta z \, ,$$

$$a_S = \rho_s d_s \Delta x \Delta z \, ,$$

$$a_T = \rho_t d_t \Delta x \Delta y \, ,$$

$$a_B = \rho_b d_b \Delta x \Delta y \, ,$$

$$a_P = a_E + a_W + a_N + a_S + a_T + a_B \, ,$$

$$b = \frac{(\rho_P^0 - \rho_P)\Delta x \Delta y \Delta z}{\Delta t} + [(\rho u^*)_w - (\rho u^*)_e]\Delta y \Delta z + [(\rho v^*)_s - (\rho v^*)_n]\Delta x \Delta z + [(\rho w^*)_b - (\rho w^*)_t]\Delta x \Delta y$$

The SIMPLE algorithm will follow on these steps:

1. Guess the p^* value
2. Solve the discretized momentum equations for u^*, v^*, w^*
3. Solve the pressure correction equation for p' and calculate p
4. Calculate u, v, w from the velocity-correction formulae, they are

$$u_e = u_e^* + d_e(p_P' - p_E') \,,$$

$$v_n = v_n^* + d_n(p_P' - p_N') \,,$$

$$w_t = w_t^* + d_t(p_P' - p_T') \,,$$

5. Solve the other discretized transport equations
6. Set the calculated p and a new p^*
7. Repeat from step 2 to 6 until the solution is converged

All the model solvers are ready. Next step, they will be used for validation of the codes to make sure that the results from genuine cases are realizable and reliable.

3.5 NUMERICAL MODEL VALIDATION: FREE DISC FLOW

A fluid flow above a disc spinning within a stagnant freestream is called free disc flow. As this flow is likewise induced by the rotation of disc, it is chosen to be a base case for code validation. The cylindrical geometry is constructed with unstructured mesh, as presented in Figure 3.1, for a free disc flow calculation. The computation region has a diameter of 1 m and a height of 1 m. The mesh is refined at the bottom region in axial direction, to accurately capture the flow profile. The validated case setup will follow the work of Ong and Owen [13].

All boundaries are set to ambient pressure, except the bottom which is a rotating wall with no-slip condition. The bottom disc rotates by 40 rad/s and the fluid has a constant density and dynamic viscosity of 1000 kg/m^3 and 0.001 kg/m-s respectively. This free disc flow is assumed to be steady flow. The compared results at local radial Reynolds number of 272000, which is in the laminar flow region, shown in Figure 3.2.

The computed results show good reliability compared to the former experimental and numerical results. Thus, the modelling of fundamental conservation equations and the numerical scheme used is assured before moving to the next step.

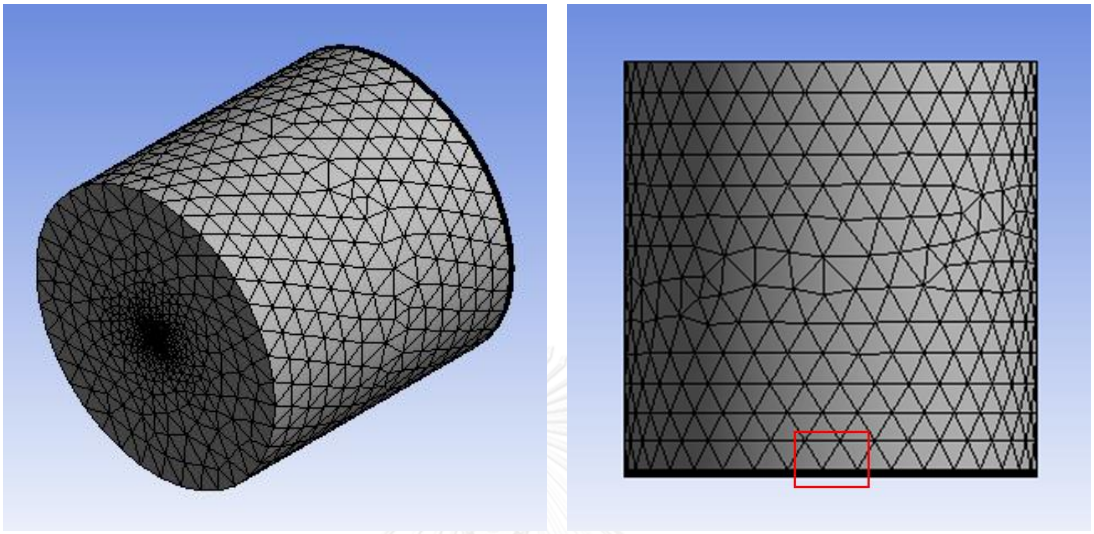

(a) *(b)*

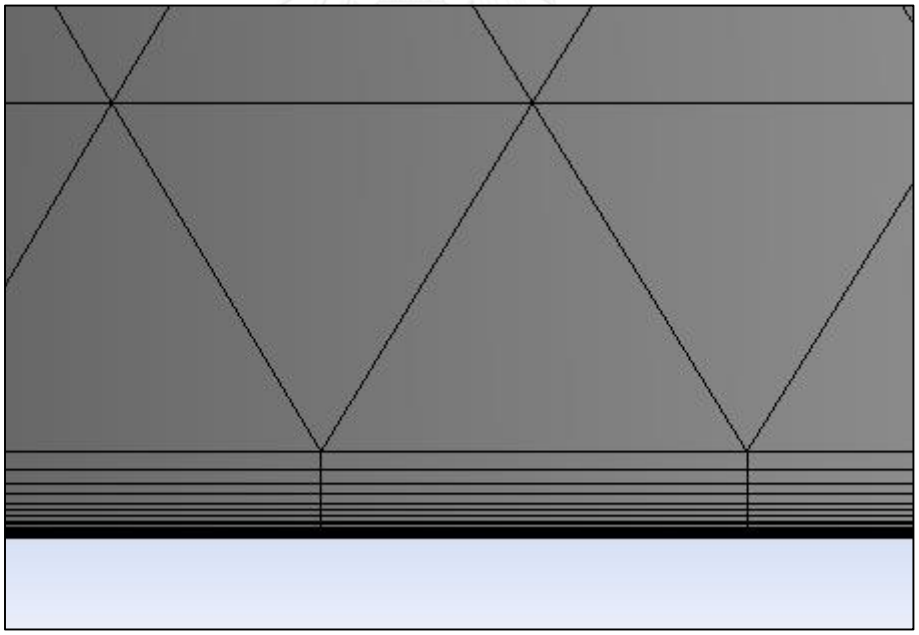

(c)

Figure 3.1 The mesh used for free disc flow validation (a) isometric view (b) side view (c) refined region within the box as shown in Figure 3.1b.

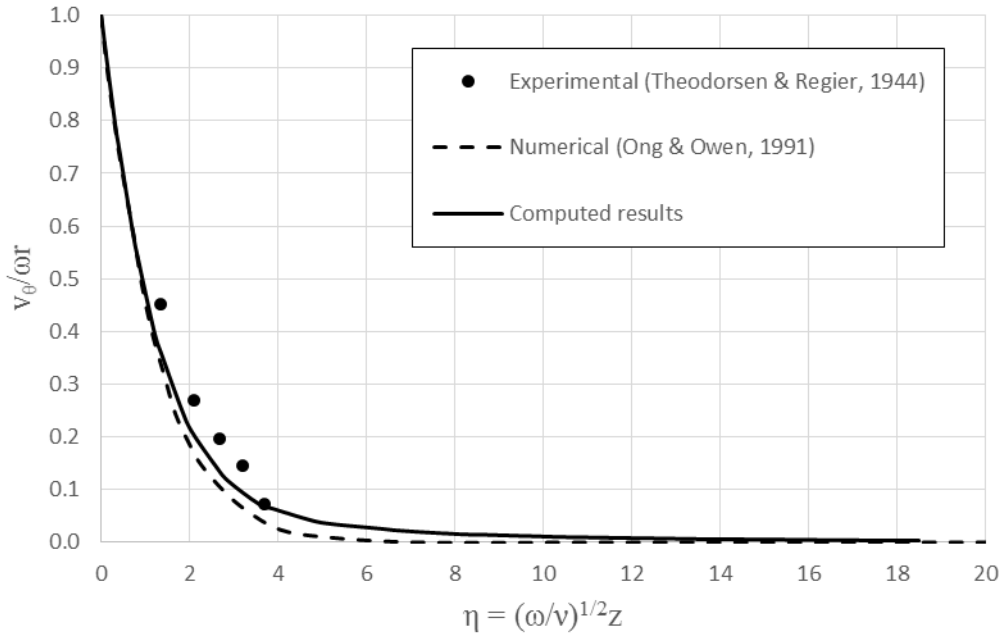

Figure 3.2 The plot of non-dimensional tangential velocity profile versus normalized axial direction at local radial Reynolds number 272000 [13, 14]

3.5 NUMERICAL MODEL VALIDATION: THIN FILM FLOW ON A DISC

Apart from the previous, the VOF model will be combined with the fundamental fluid dynamics model. To validate the VOF model and Compressive scheme, the flow of thin liquid film on a spinning disc is appointed as a simulation case, which of the physics is very close to this work cases.

The experimental work of Leshev and Peev [15] is followed. The 40-cm-diameter disc is made of aluminum with smooth surface finishing. Water is injected on the rotating disc and spread as liquid film over the disc. The water film height is measured by the needle probe method. The validated case uses the water flow rate of 5.33 mL/s and rotates the disc with the speed of 10.47 rad/s, or approximately 100 rpm. From the information above, the applied boundary conditions for numerical validation are summarized in Figure 3.3.

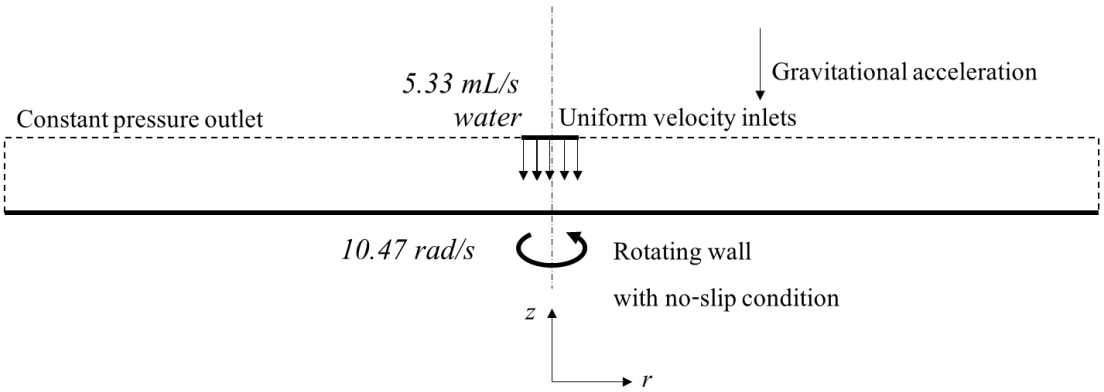

Figure 3.3 Boundary conditions of film flow validation

Moreover, some old works have studied the liquid film height analytically. They derived expressions from the momentum equation for calculating the film height. To simplify the derivation, the inertial force, body force, friction and surface tension with air are neglected. The expressions are from Lepehin and Riabchuk [16] (Math model I) and Rauscher et al. [17] (Math model II), which are respectively stated by

$$\delta = 0.886 Q^{0.348} \nu^{0.328} \Omega^{-0.676} r^{-0.7} \tag{3.9}$$

and

$$\delta = 0.782 Q^{0.333} \nu^{0.333} \Omega^{-0.667} r^{-0.667} \tag{3.10}$$

These expressions have already compared with the experimental results of Leshev and Peev [15] and presented good compatibility. Water and air surface tension will not be included in the numerical model validation, forasmuch the expressions evinced its insignificance. The computed results are compared with the experimental and analytical results in Figure 3.4.

As already seen, the computed solution acts some overshoot and undershoot at the inner radius range but get along well with the other results beyond that range. Therefore, including of VOF model in the simulation is assured its validity. Besides, the surface tension in this film flow is found to be negligible. Consequently, difficulty of the computation in the next chapter can be reduced by this negation.

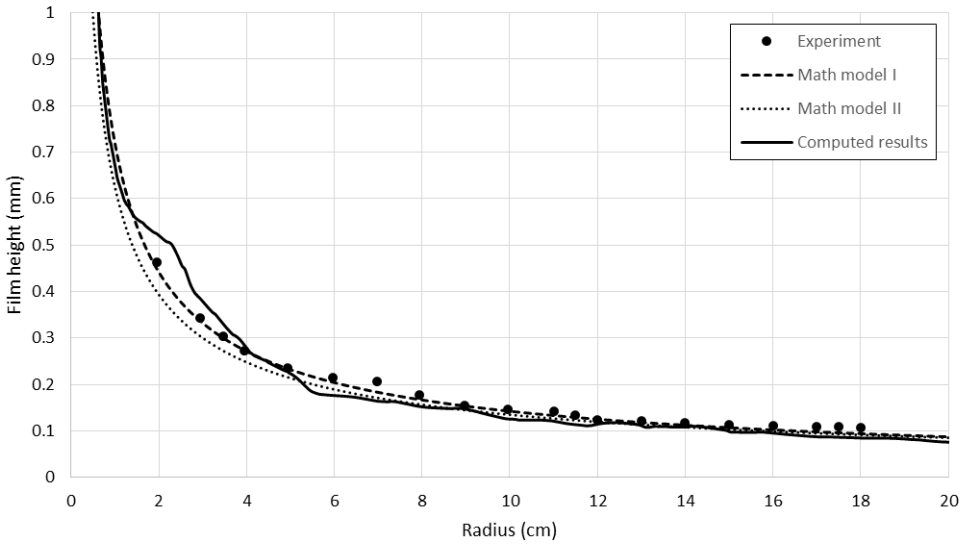

Figure 3.4 The comparison of film height profiles from the computed results and former works

CHAPTER 4
CASE SETUPS AND RESULTS

The previous chapter has presented related theories, mathematical models and numerical model validations which help ensuring reliability of the numerical codes. Thereby, now, all parts of the model already proposed will be used for solving the intended case of two immiscible liquids mixing in an SDR. The results from all computations will be discussed in this chapter.

4.1 DOMAIN GEOMETRY AND BOUNDARY CONDITIONS

The SDR investigated here has two inlets on the top which each injects different kind of immiscible liquid. A spinning disc is at the bottom receiving the liquid streams for mixing. The mixture exits the reactor at the edge of disc. The reactor casing is not totally closed, there will be air from the outside of SDR enclosing the liquid phase during processing. The geometry for determining the flow must be three-dimensional, because of asymmetry of the flow.

Dimensions of the SDR configuration are illustrated in the Figure 4.1. Both liquid feedings, with diameter of 10 mm, are symmetrically shifted from the disc center by 20 mm. The different immiscible liquids are injected vertically above the disc surface by 3 mm. The spinning disc has a diameter of 410 mm. Thus, a flat cylindrical geometry, with 3 mm thickness, for the calculation is created with two circular holes shifted equally from the rotating axis at the top. The computational region does not take place beyond the edge of disc and is assumed to be open air, in order to focusing only on the effect from the disc, although the SDR has a stationary casing actually. Unstructured mesh with 132759 cells is used for calculations, as shown in Figure 4.2.

This study uses water and n-heptane for simulating mixing flow in the SDR. For the simulation, three phases exists in the domain; air, water and n-heptane, which of properties are listed in Table 4.1. Air is chosen to be the primary phase. Velocity-inlet boundary conditions are applied for prescribing uniform velocities for both inlet holes. Each value of velocities is according to the given flow rates. The bottom boundary which represents the spinning disc is modelled as a smooth rotating wall with no-slip

condition. The remaining boundaries are set to ambient pressure and air can enter the calculation domain through these boundaries. The gravitational body force is included in this calculation, but surface tensions between all fluids are neglected. The summary of boundary conditions is illustrated in Figure 4.3.

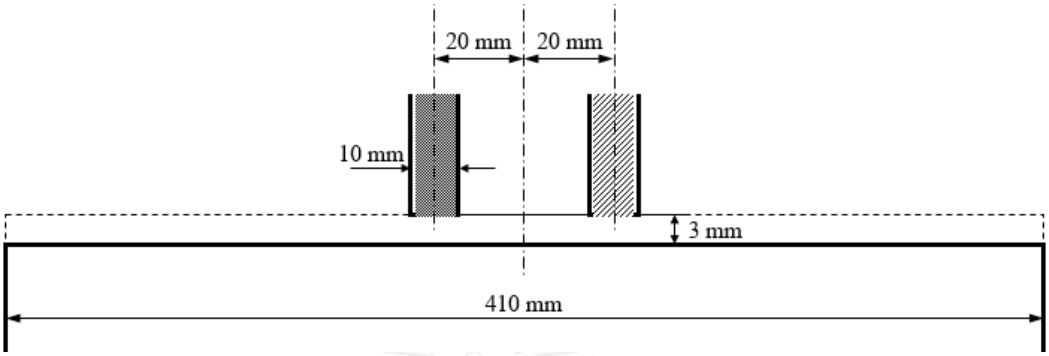

Figure 4.1 Dimensions of the SDR geometry

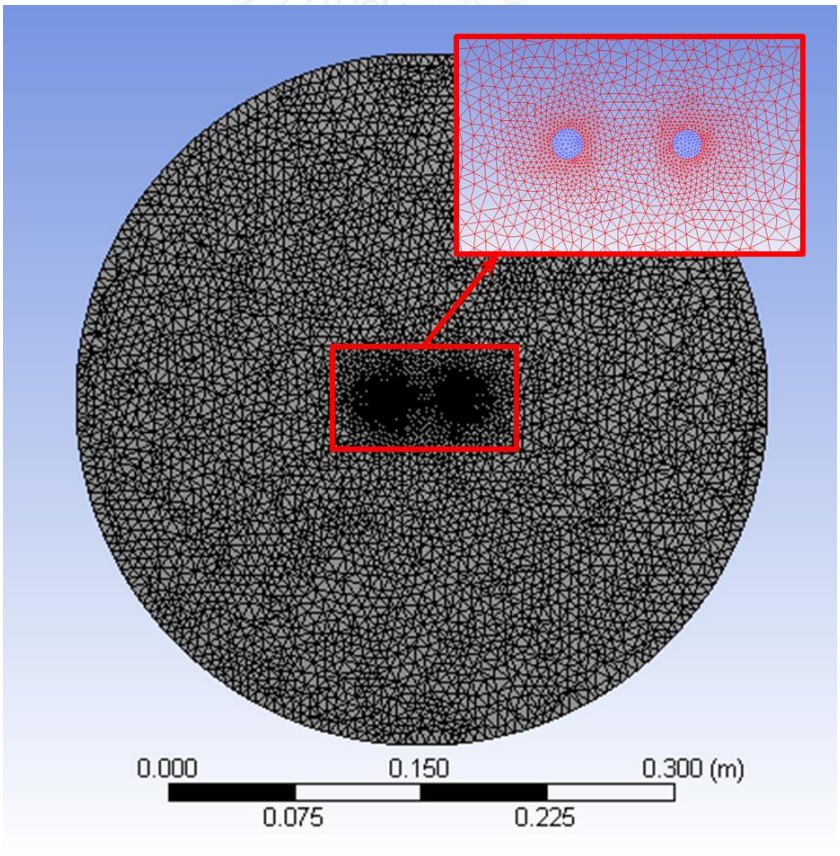

Figure 4.2 Unstructured mesh used in the simulation

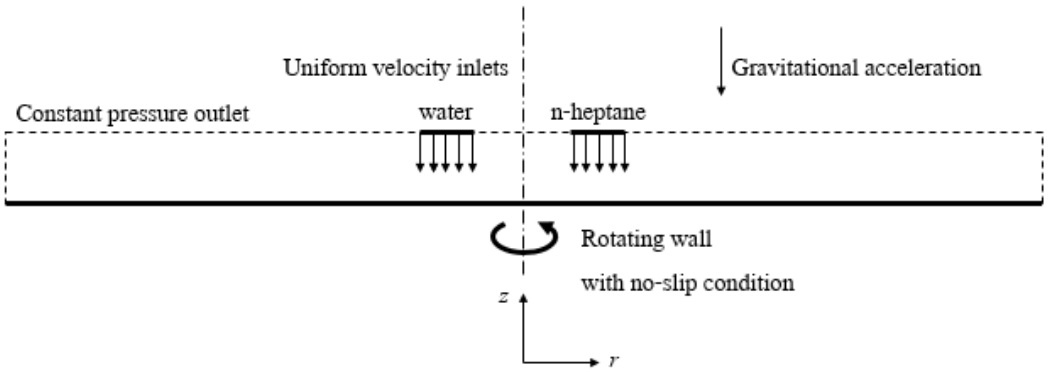

Figure 4.3 Boundary conditions of flow domain

Table 4.1 Properties of fluids in the study

Fluid	**Density (kg/m^3)**	**Dynamic viscosity (kg/m-s)**
water (liquid)	1000	1.00×10^{-3}
n-heptane (liquid)	684	4.09×10^{-4}
air	1.225	1.7894×10^{-5}

The flow rates of both liquids are set to 5.330, 7.854 and 15.708 mL/s equally for each study case. The rotating speed of disc varies from 10 to 2500 rpm. Next step, the simulation cases will be calculated and the effects of volumetric flow rate and rotating speed are evaluated. After that, in addition, cases of unequal volumetric flow rates of both liquids, inlet position shifting, and amount of feeding inlets are also studied their effects.

4.2 EFFECTS OF ROTATING SPEEDS AND LIQUID FLOW RATES

After done all simulation cases, many interesting points are pending to be picked from the results. However, the simulations of rotating speeds 10, 1000 and 2500 rpm were diverged and will not be determined, which will be explained later. As for the converged solutions, interfacial area, mean residence time of each phase, liquid film height distributions and contours of each liquid volume fraction will be extracted from the simulations and discussed.

4.2.1 Interfacial area between two immiscible liquids

As quality of mixing directly indicates amount of mass transfer or reaction rate, interfacial area between water and n-heptane is chosen to be a mixing representative. It was proved that the regions of high reaction rate are coincided with the contact region of two reactants [3]. Moreover, expansion of the interfacial area also enhances mass transfer rate, stated by

$$\dot{n}_i = k_L A \Delta c_i \tag{4.1}$$

which is analogous to convective heat transfer rate, given by Newton's law of cooling:

$$\dot{q} = hA\Delta T \tag{4.2}$$

Pragmatically, there are no instruments that can measure the interfacial area directly. Thus, interfacial area in Eq. 4.1 is commonly coupled with the mass transfer coefficient and determined as one coefficient in the form of $(k_L A)$. The rate of mass transfer and concentration difference can be measured experimentally and used for calculating $(k_L A)$. Fortunately, from the numerical study methodology of this work, the interfacial area can be calculated directly from the solutions.

To compute the interfacial area, first, consider a stratified two-phase system in Figure 4.4. The region which occupied by a phase, other phases cannot exist. However, since the volume fraction is modelled as a continuous function, there must be gradient of volume fraction (the green region in Figure 4.4 which the values of volume fraction are between zero and unity, $0 < X_i < 1$) occurs along the phase boundary or contacting region. Ideally, thickness of the boundary between phases is infinitesimal, or assumed to be absolutely thin as if the thickness is zero. Nevertheless, the gradient region being displayed within the resultant volume fraction field definitely contain finite thickness, which is not enough to certainly represent the phase boundary. In the two-phase system which contains phase A and phase B, the volume fraction of phase A is the complement of phase B volume fraction in unity, by Eq. 3.4. This relation can be written as

$$X_A = 1 - X_B$$

Therefore, the points which have phase A volume fraction of 0.5, phase B volume fraction must also be 0.5 at these points. For simplicity of determination, the phase

boundary is defined here to be a surface with the phase volume fraction of 0.5, also called a half volume fraction surface. However, before advancing to the interfacial area calculation step, remember that this assumption is constructed from two-phase system.

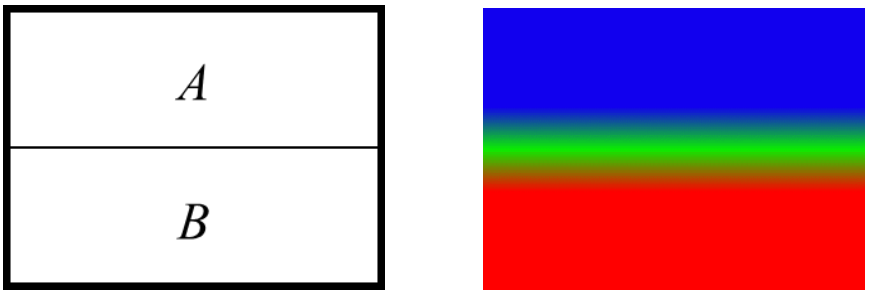

Figure 4.4 A stratified two-phase system containing phase A and B

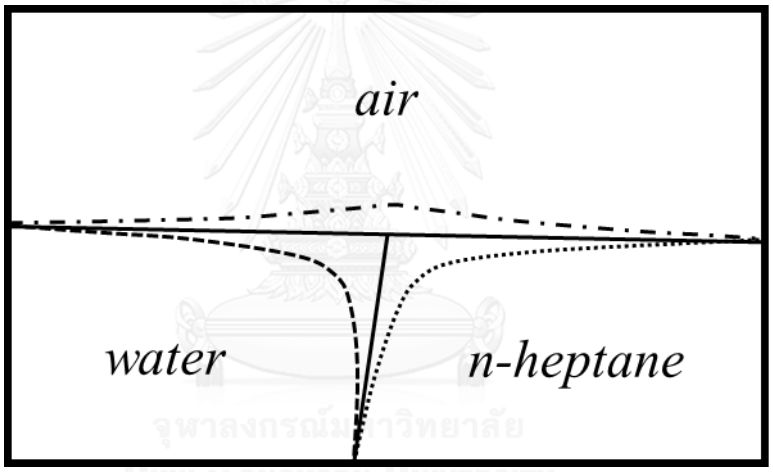

Figure 4.5 The phase boundaries between water, n-heptane and air, and the half volume fraction surfaces of each phases

Although the interest in this work is about mixing between two liquids, there are three fluids involved in the flow inside the SDR, water, n-heptane and air. Hence, the flow is considered as three-phase system, which is more complex than the two-phase. A feature which have to be taken into account in addition to two-phase system is three-phase contacting region, as demonstrated in Figure 4.5. The phase boundaries that partitioning the three phases could not be specified from the numerical solutions forthrightly as two-phase system. The trouble is faced within the volume fraction gradient region between three phases. The volume fractions of all phases cannot be 0.5 simultaneously, since the sum of three volume fractions must not exceed unity. Thus,

the assumption about tracing along the surface of 0.5 volume fraction to impose the phase boundaries is invalid here. However, albeit the interphase boundaries could not be prescribe clearly in three-phase system, the interfacial area in this problematic zone can still be calculated by approximation.

As determining from Figure 4.5, the surfaces with a half volume fraction of any fluids are coincided only in pair at the contacting boundary between any two phases. The surfaces of any fluid volume fraction of 0.5 eventually deviate from the three-phase contacting region. Although the half volume fraction surfaces of every fluids are not the real phase boundaries, the surfaces at least can be used for estimating the interfacial area between water and n-heptane. The area magnitude of any half volume fraction surfaces (σ) can be calculated by the software. Then, to approximate the interfacial area, the computed area magnitudes of the surfaces are substituted in this formula,

$$A_{w/h} \approx \frac{1}{2}(\sigma_w + \sigma_h - \sigma_a) \tag{4.3}$$

Consequence by the operating conditions which give a high value of interfacial area are sought. Figure 4.6 shows the computed interfacial areas from Eq. 4.3 at various rotating speeds and flow rates. Increasing rotating speed explicitly decreases the interfacial area. The area in the range of 0.052-0.064 m^2 drops to 0.005-0.016 m^2 as the rotating speed is changed from 50 to 250 rpm. However, the contacting area can be increased by injecting more flow rate, but this manner is still not strong as rotating speed changing.

4.2.2 Mean residence time

Another remarkable performance of an SDR is residence time, which imply the time taken in the reactor for one input material. The mean residence time (t_m) is defined as

$$t_m = \frac{volume\ occupied\ in\ the\ system}{inlet\ volumetric\ flow\ rate} \tag{4.4}$$

Short residence time is preferred for any chemical reactor. The residence time is calculated for each immiscible liquid and the results of water and n-heptane are illustrated in Figure 4.7 and 4.8, respectively. Regardless of which liquid is being

determined, they have a same trend of variation. The residence times decrease by increasing rotating speed, as the same manner for all volumetric flow rates.

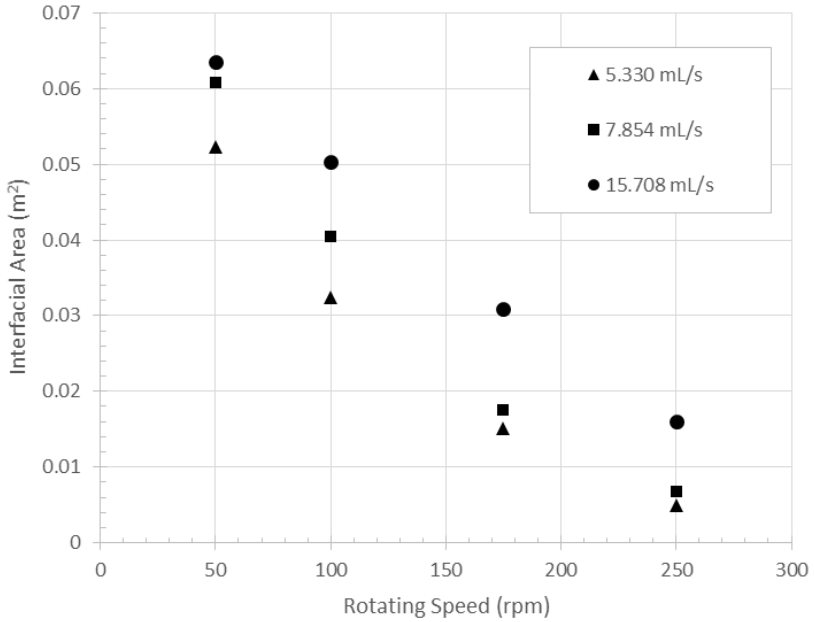

Figure 4.6 Interfacial area between water and n-heptane with the rotating speeds of 50 to 250 rpm and the flow rates of 5.330, 7.854 and 15.708 mL/s

However, the residence time is found to be sensitive to rotating speed at the low speed range. For example in the case of 15.708 mL/s flow rate, the mean residence time of n-heptane drops from 1.17 to 0.82 s when the rotating speed is accelerated from 50 to 100 rpm. On the other hand, the change of rotating speed from 175 to 250 rpm causes little decrease on n-heptane residence time from 0.61 to 0.50 s. This low speed range effect is intensified if the SDR is operated at the low input flow rate of water and n-heptane, which is 5.33 mL/s each in this present work. As seen in Figure 4.7, the mean residence time of water steeply drops by 1.29 s in the low speed, while the high speed range only drops by 0.34 s. Also, from Figure 4.8, the residence time of n-heptane in the range of 50 to 100 rpm drops by 0.75 s, which is approximately four times of the high speed range, 0.20 s.

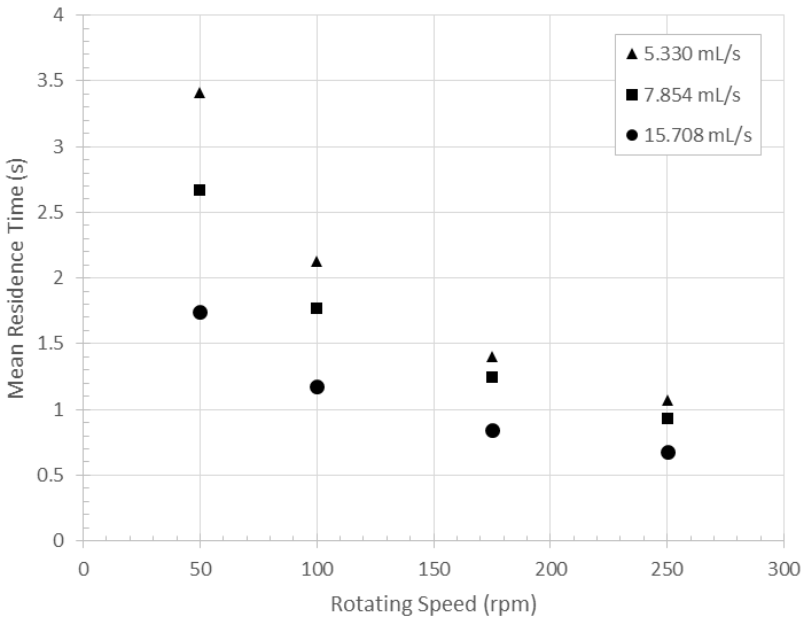

Figure 4.7 Mean residence time of water liquid with the rotating speeds of 50 to 250 rpm and the flow rates of 5.330, 7.854 and 15.708 mL/s

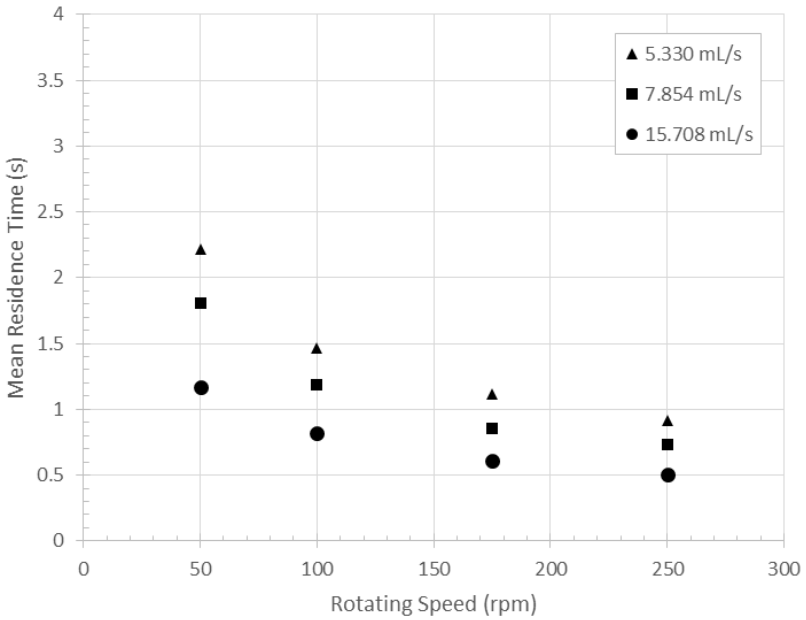

Figure 4.8 Mean residence time of n-heptane with the rotating speeds of 50 to 250 rpm and the flow rates of 5.330, 7.854 and 15.708 mL/s

By varying flow rates at any constant rotating speed, the mean residence times decrease as the input flow rates increase. However, the effect of low range rotating speed still exists for the change of flow rate at a constant rotating speed. Less the rotating speed, more the change of residence time by input flow rates. Likewise, the

residence times of water and n-heptane drop by 1.67 and 1.04 s at 50 rpm, when the both liquid flow rates are adjusted from 15.708 to 5.330 mL/s. Nevertheless, the residence times of both liquids just drop by 0.39 and 0.42 s at 250 rpm.

Another interesting point is the residence time of n-heptane always shorter than water in all cases, although both liquids are fed at the equal volumetric flow rate and shifted position from the disc center. However, as mentioned early, the residence times of water and n-heptane still share the same pattern. Thus, the residence times of both liquids are plotted and compared for all 12 cases, which of the solutions are converged, in Figure 4.9. It reveals such an interesting correlation between both liquids. The plots are fit with a straight line, which can be expressed by linear equation as

$$t_{m,heptane} = (0.6853)t_{m,water} \tag{4.5}$$

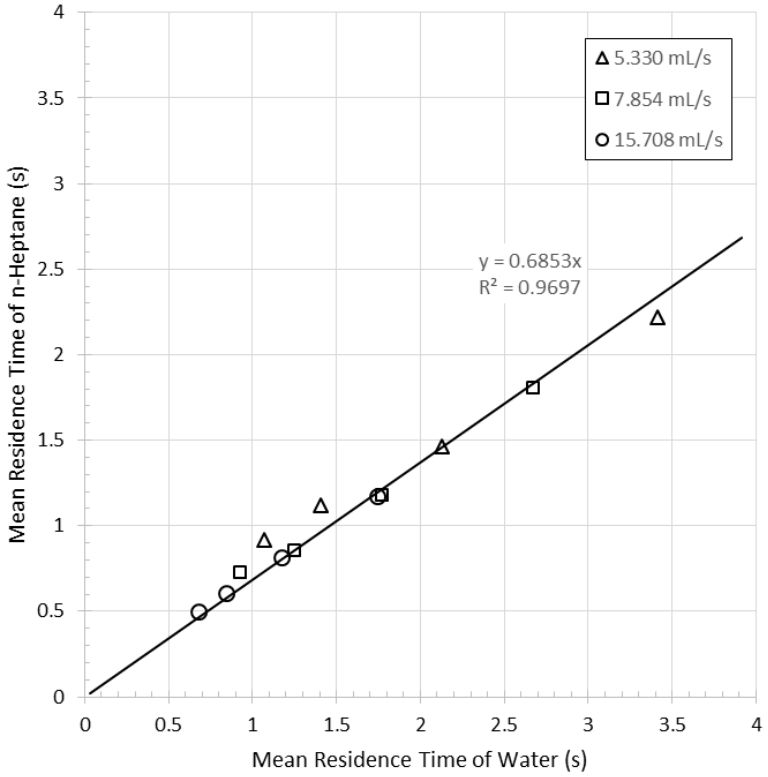

Figure 4.9 Correlation between mean residence time of water and n-heptane

It means, the residence time of n-heptane relates proportionally with water, and the ratio of n-heptane residence time to water residence time is discovered to be 0.6853 approximately. Hence, if a residence time of either liquid is known, another one can be predicted by Eq. 4.4.

Since n-heptane always has the mean residence time less than water, the different between physical properties of two liquids should be the main factor. Due to density and viscosity of n-heptane which are all lower than water, see Table 4.1, thus, n-heptane has lesser inertia, which makes it thrown out of the disc easier, and low viscosity to hold in the reactor.

4.2.3 Liquid film height distributions

Water and n-heptane are mixed together on the rotating disc and driven radially to the disc edge in the form of liquid film. Descriptions of film should be collected here since there are not much old works discussed about. Arbitrary positions on the disc are located with polar coordinates (r and θ), as shown in Figure 4.10. First, the film heights at different constant radii are circumferentially averaged from all cases. The averaged data is plotted and observed to two aspects, varying rotating speeds at constant flow rate (Figure 4.11-4.12) and varying flow rates at constant rotating speed (Figure 4.14-4.16).

The similarity of average film height can be noticed from radius of 6 cm to the edge of the spinning disc, from Figure 4.11-4.12. The height decreases as the rotating speed increases. However, it seems like the local change is acute only in the low speed range, whereas the speed changing at high rotating speeds does not make the height significantly change. Furthermore, the radial distribution of average film height is flatten when the rotating speed increases. Thus, to keep uniformity of mixing liquid film thickness for some purposes, The SDR should be operated at the high rotating speeds.

Figure 4.13 explicitly illustrates why the average film heights at radius of 3 cm from the center are not included in the aforementioned similarity. The heights are rather close to each other, although the rotating speed is changed. Also, they are very high when compared to other liquid film thickness at a further radius. It can imply that the effect from rotating speed cannot dominate the mixing liquid film height at the inner radius. From another point of view, maybe, the excess height of film is occurred by newly impinging input liquids, because the position is very near the liquid feeders.

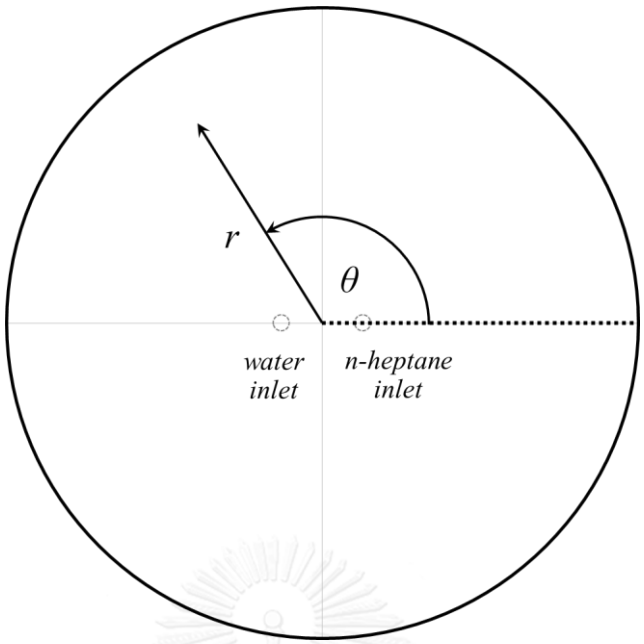

Figure 4.10 Polar coordinates attached with rotating disc

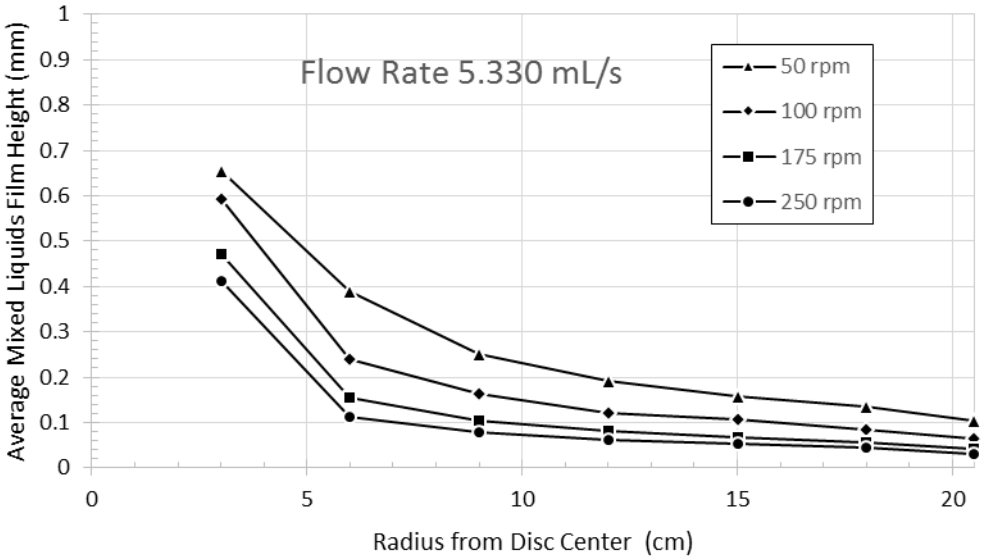

Figure 4.11 Average film thickness with the liquid flow rate of 5.330 mL/s each

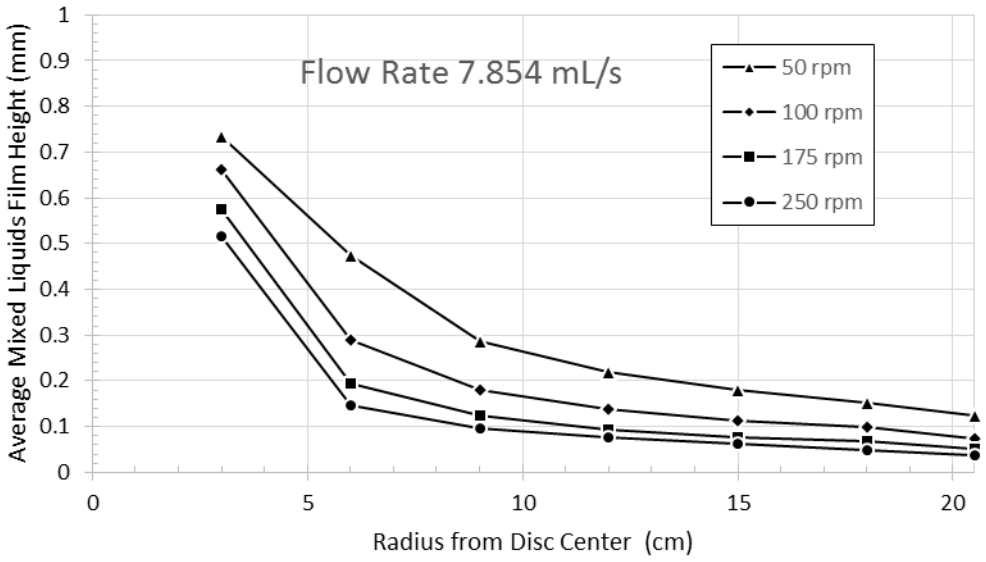

Figure 4.12 Average film thickness with the liquid flow rate of 7.854 mL/s each

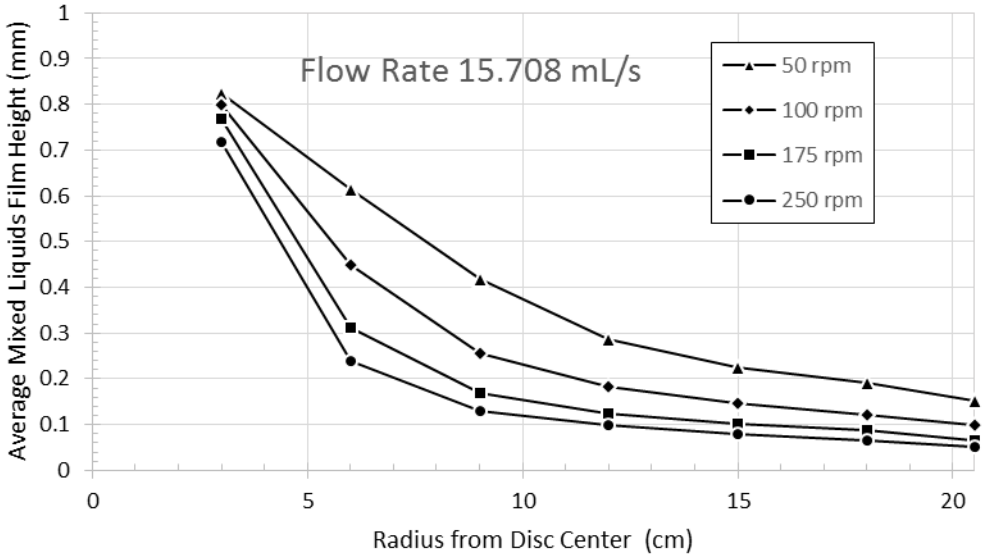

Figure 4.13 Average film thickness with the liquid flow rate of 15.708 mL/s each

For the fixed rotating speed aspect, the liquid flow rates of both water and n-heptane are also found to have an influence on the average liquid film height. Nevertheless, this influence is less significant when the SDR is operated at 250 rpm.

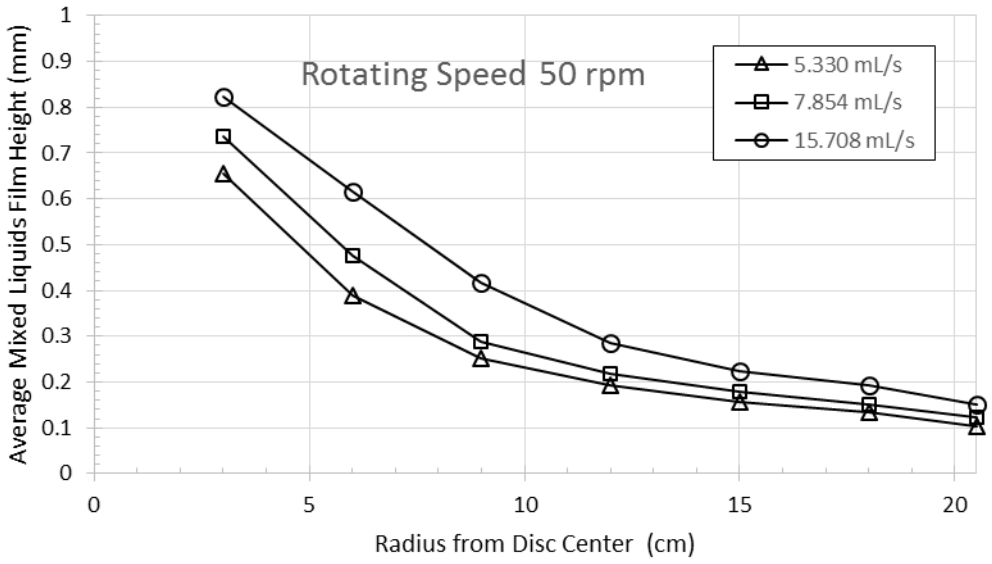

Figure 4.14 Average film thickness with the rotating speed of 50 rpm

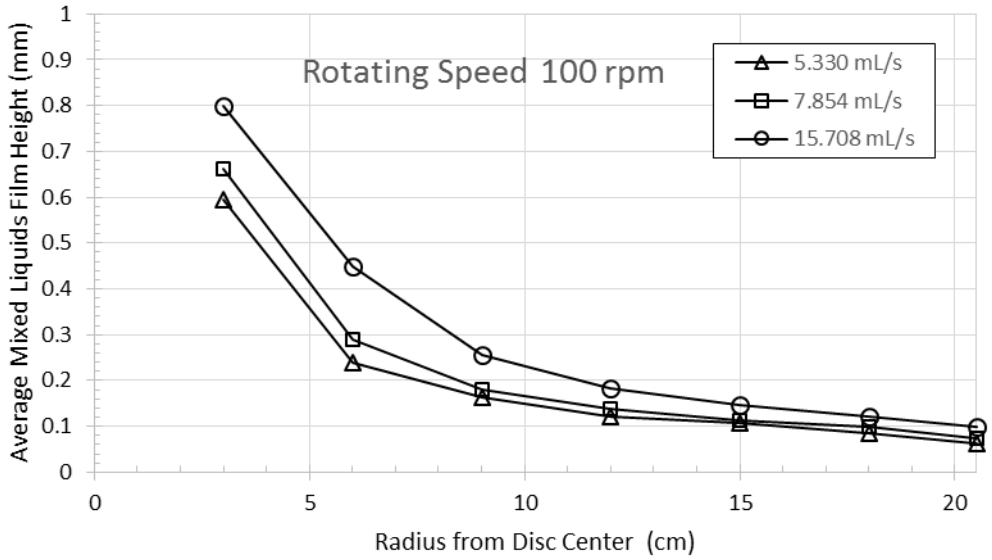

Figure 4.15 Average film thickness with the rotating speed of 100 rpm

Moreover, the average film height can imply the volume occupied by mixing liquids inside the SDR. That means, from Eq. 4.3, the film height is proportional to liquid residence time, when the liquid flow rates remain constant. However, the high mixing liquid film height cannot imply that the mean residence time is high too. Sometimes, high films come from large amount of flow rate, which can make residence time short.

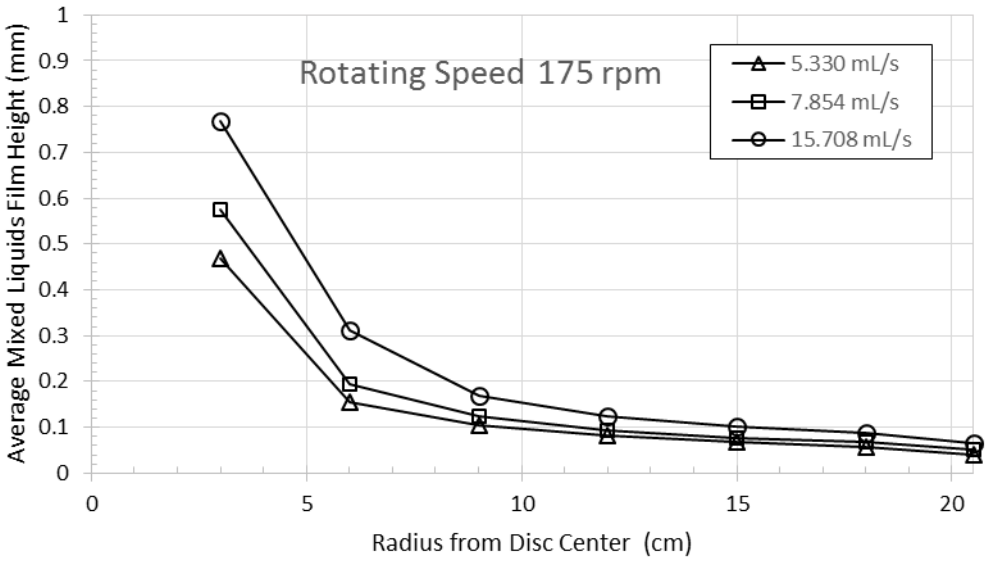

Figure 4.16 Average film thickness with the rotating speed of 175 rpm

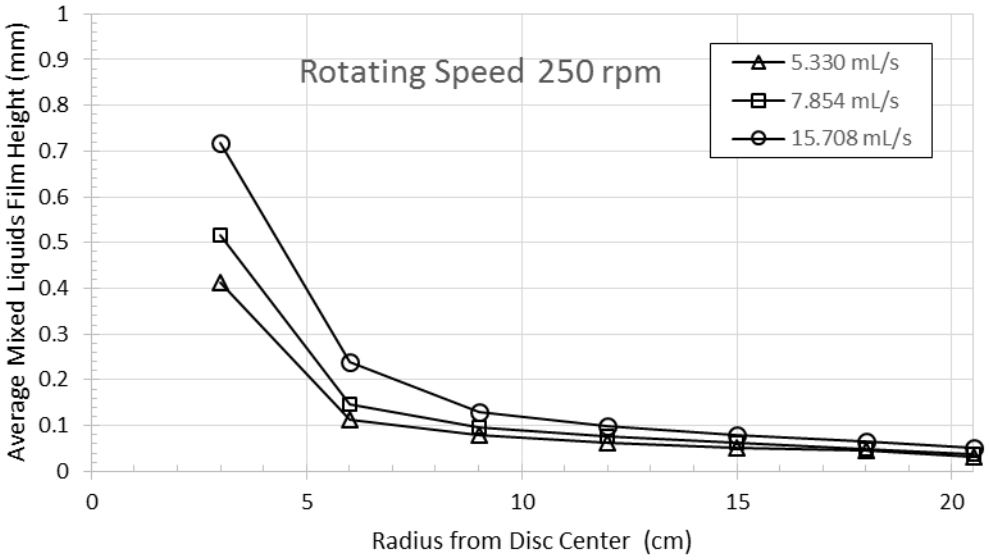

Figure 4.17 Average film thickness with the rotating speed of 250 rpm

To visualize the film more clearly, the actual film height profiles are distributed in angular view at various constant radii. The cases of 50 and 250 rpm with the flow rate of 15.708 mL/s are picked up for examples, as shown in Figure 4.18 and 4.19. The film inconsistency of 50 rpm case can be caught obviously, whereas the 250 rpm case

is insignificant. That means, more the rotating speed, uniformity of film thickness is gained.

4.2.4 Phase contour

To visualize the mixing flow inside the SDR, phase contours of both liquids are revealed at various constant height cross-sections, including at disc surface and 10, 20, 30, 50, 75, 100, 200 and 400 μm above the disc. The cases of 15.708 mL/s flow rate with rotating speed of 50 and 250 rpm, which give the highest interfacial area and lowest residence times of both liquids respectively, are chosen to be examples, as shown in Figure 4.20 to 4.25. Normally, at the region near the spinning disc, phase contours of n-heptane are inverse or negative of water phase contours. They display the same pattern but the colors are opposite (the region which of color of water contour is red, for n-heptane contour is blue). That means, these cross-sectional contours are within the mixing liquid film, where of the region that water exists, n-heptane does not.

Air phase cannot be found in the contours until the height of cross-section layer is beyond the liquid film thickness. The region in the contours where air occupies is coincident with the region which water and n-heptane both vanish. This region can be observed by comparing water contour with n-heptane contour at the same layer and matching blue region at the same position. The air region gradually appears as the contour layer is higher. It begins to occur at the disc edge and internally spread to the center.

Next, the case of the shortest mean residence time are discussed its contours at various layer. At the bottom layer, Figure 4.20a, the rotating disc is covered by mixed liquid film throughout. Most of the space is held by water, and the rest is n-heptane which appears around the near-center region and outer region. As the cross-section steps higher, n-heptane seems to propagate from outer region to the center of disc in spiral path, by the motion of contours in Figure 4.20b-c and 4.21a-b. The air phase obviously appears at the 75 μm layer, Figure 4.21c, and swirling of both immiscible liquids is less as the cross-section height is more, Figure 4.22. Finally, the liquids only appear nearby inlet holes of each.

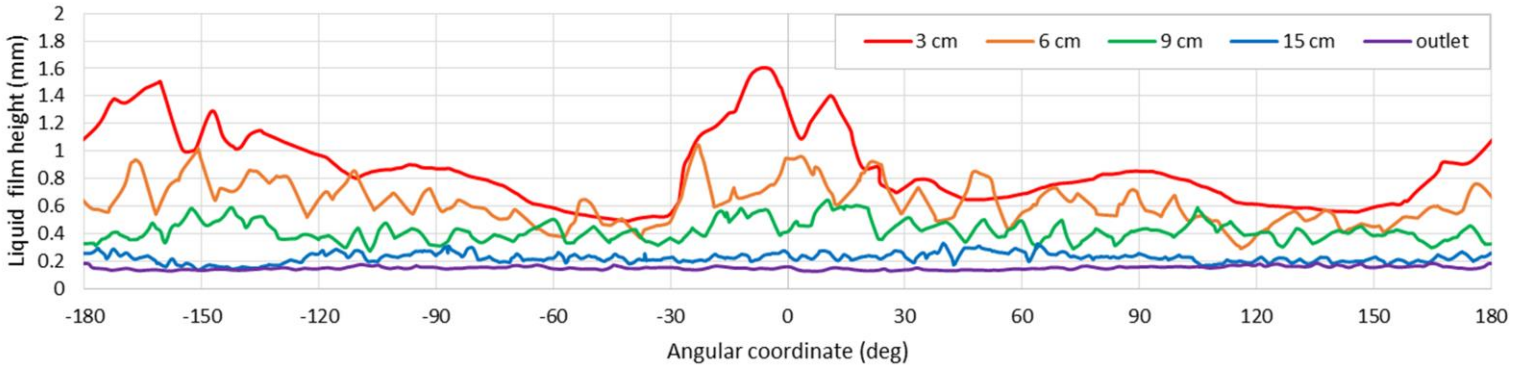

Figure 4.18 Circumferential film height profile at various constant disc radii with rotating speed of 50 rpm and flow rate of 15.708 mL/s

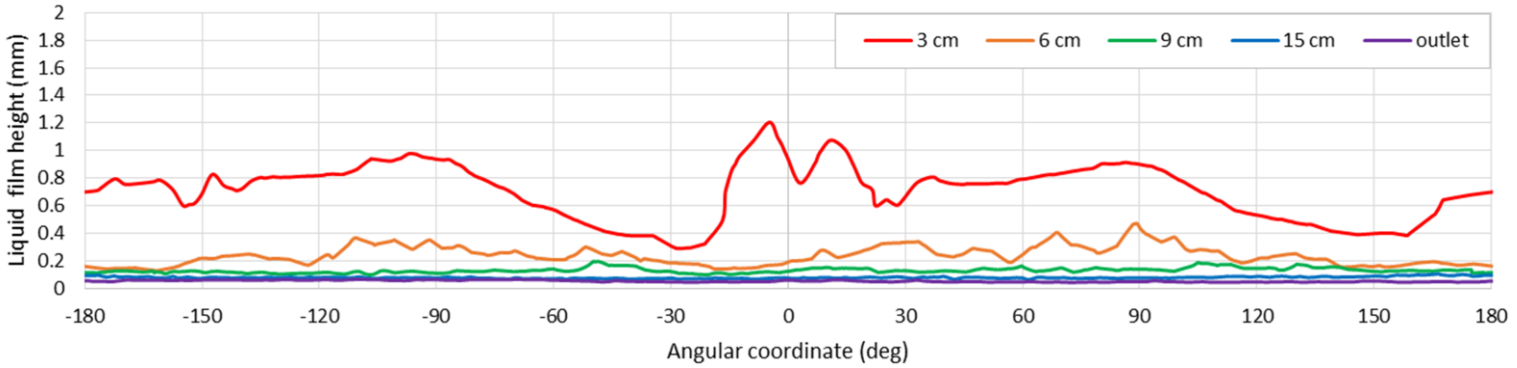

Figure 4.19 Circumferential film height profile at various constant disc radii at rotating speed of 250 rpm and flow rate of 15.708 mL/s

Next, the case of the shortest mean residence time are discussed its contours at various layer. At the bottom layer, Figure 4.20a, the rotating disc is covered by mixed liquid film throughout. Most of the space is held by water, and the rest is n-heptane which appears around the near-center region and outer region. As the cross-section steps higher, n-heptane seems to propagate from outer region to the center of disc in spiral path, by the motion of contours in Figure 4.20b-c and 4.21a-b. The air phase obviously appears at the 75 μm layer, Figure 4.21c, and swirling of both immiscible liquids is less as the cross-section height is more, Figure 4.22. Finally, the liquids only appear nearby inlet holes of each.

From another case, at 50 rpm which gives the highest interfacial area, the disc surface are also fulfilled with mixing liquids, Figure 4.23a. However, n-heptane can occupy the disc region more than the 250 rpm case. In addition, there is the part of region which n-heptane totally exists, above the disc center. The spiral path of n-heptane obviously appears without seeing the other higher layers. On the other hand, the contours have no motion as contour height increases, only the strength of contour color is changing, from Figure 4.23b-c, 4.24 and 4.25a. The first appearance of air phase can be seen from Figure 4.25b and the swirling of liquid contour at the 400 μm level is stronger than the 250 rpm case at the same height.

4.2.5 Undetermined cases

After all cases were simulated, some of them could not get the desired solution or not converge. At the very low rotating speed of 10 rpm, the solutions are diverged regardless of the input volumetric flow rates. The occurrence of solution divergence could be ascribed that hydraulic jump exists on the spinning disc during operation, since the former study about film flow on a rotating disc found at the low rotating speed [15]. Thus, these cases are out of determination because hydraulic jump causes mixed liquid film inconsistent and this situation is not desired in actual operation of SDR.

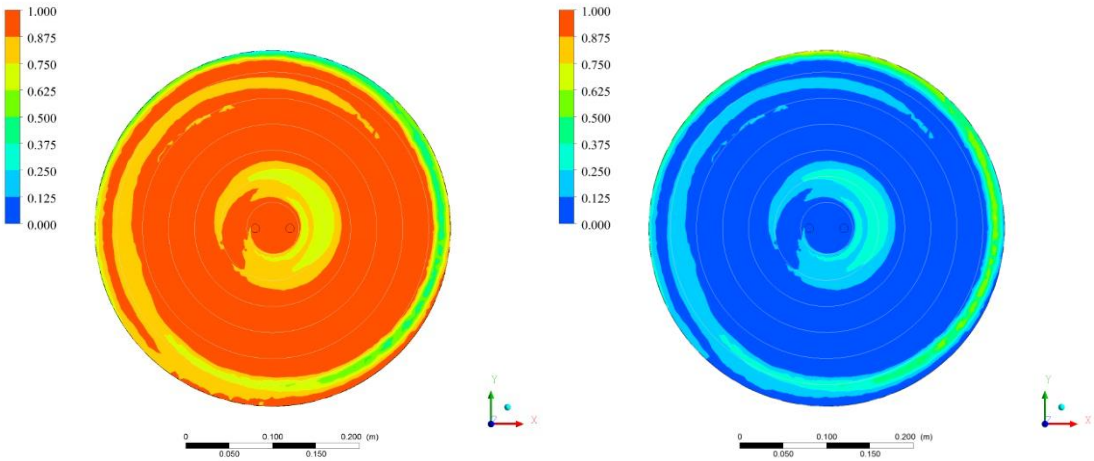

(a) at disc surface

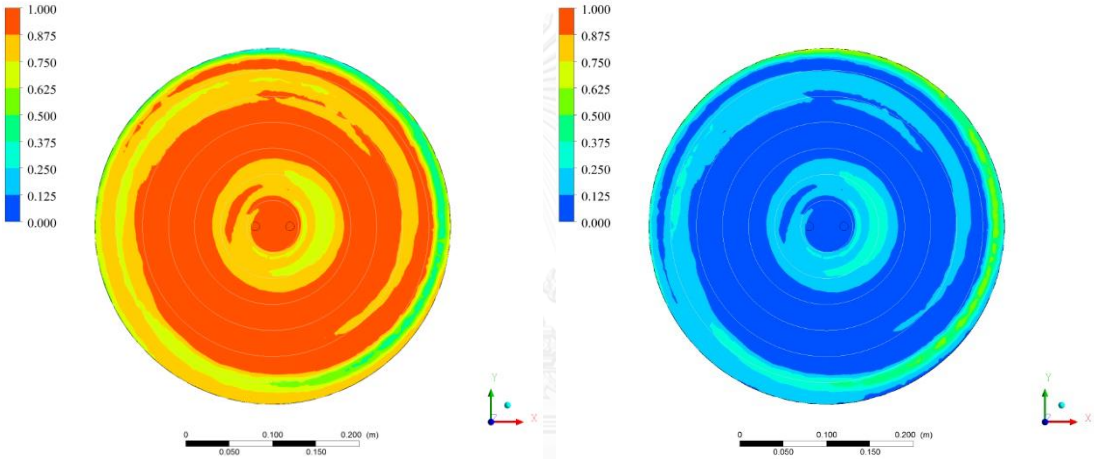

(b) 10 μm from disc

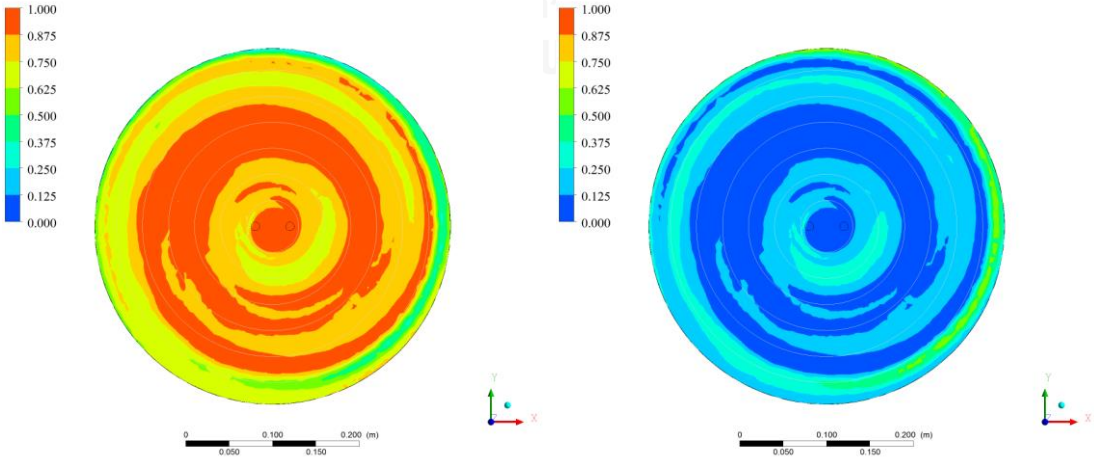

(c) 20 μm from disc

Figure 4.20 Cross-sectional volume fraction contours of water (LHS) and n-heptane (RHS) at disc surface, 10 and 20 μm with disc rotating speed of 250 rpm and both liquid flow rate of 15.708 mL/s each

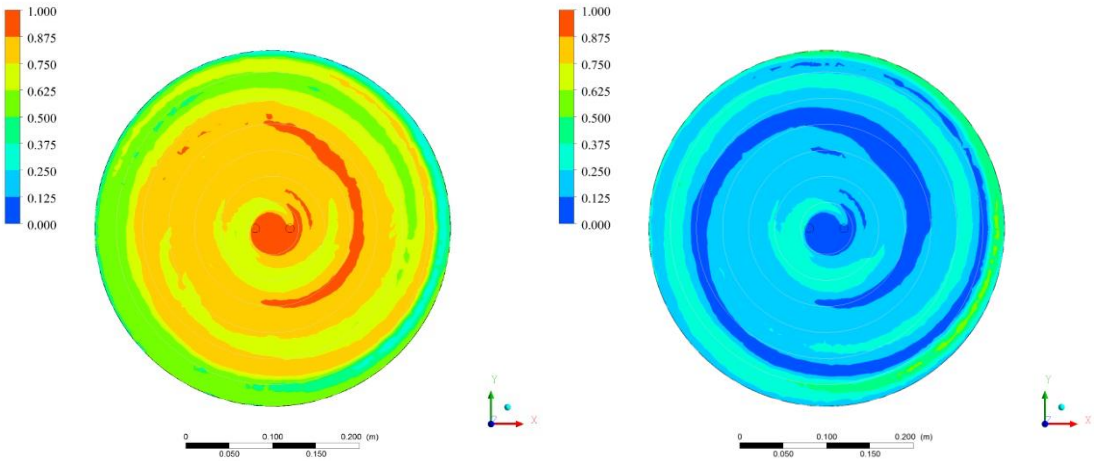

(a) 30 μm from disc

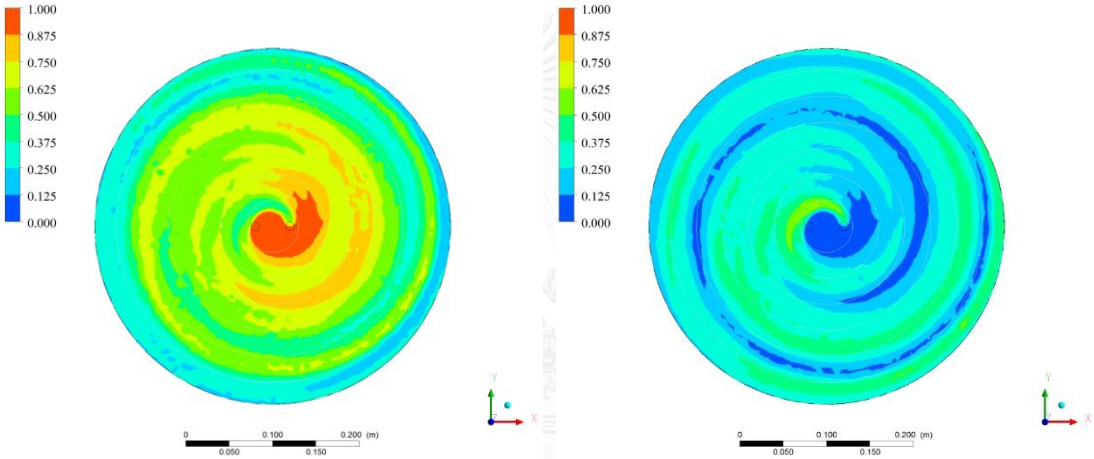

(b) 50 μm from disc

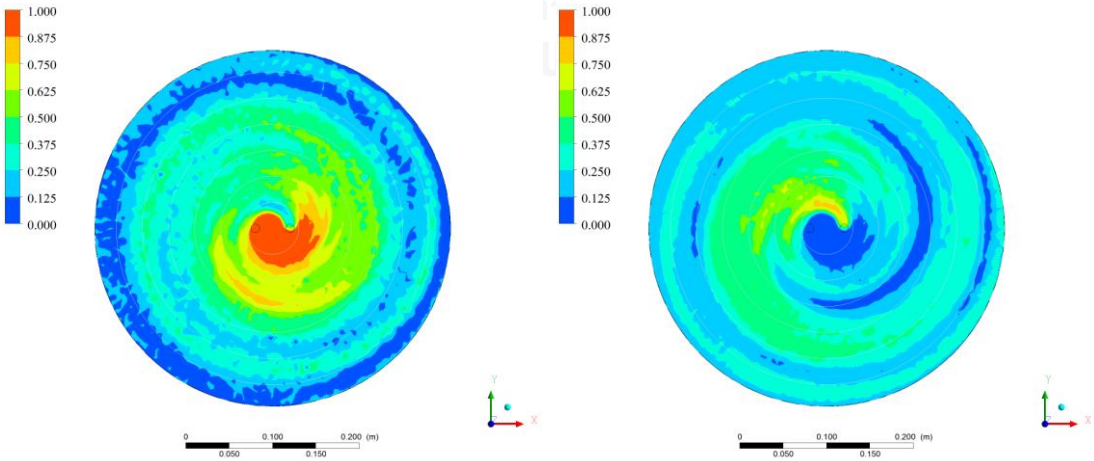

(c) 75 μm from disc

Figure 4.21 Cross-sectional volume fraction contours of water (LHS) and n-heptane (RHS) at 30, 50 and 75 μm with disc rotating speed of 250 rpm and both liquid flow rate of 15.708 mL/s each

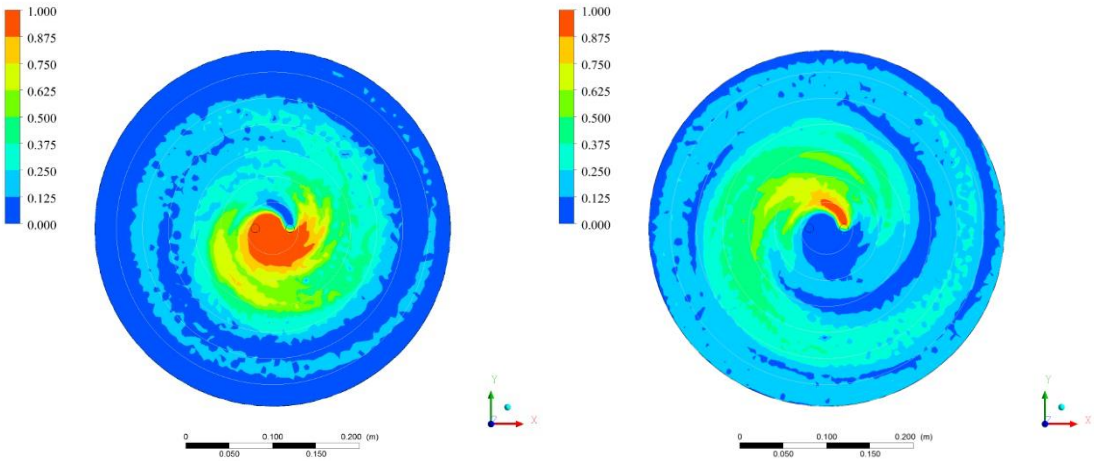

(a) 100 μm from disc

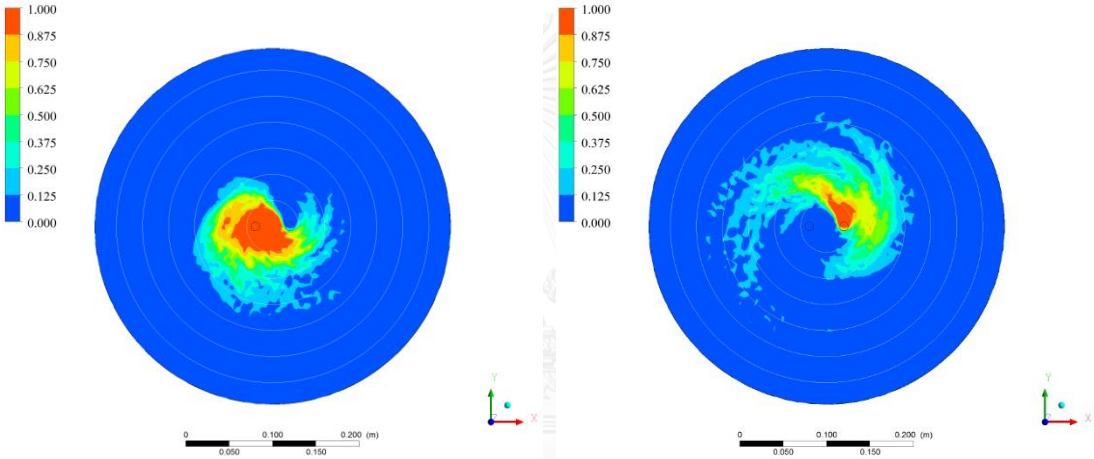

(b) 200 μm from disc

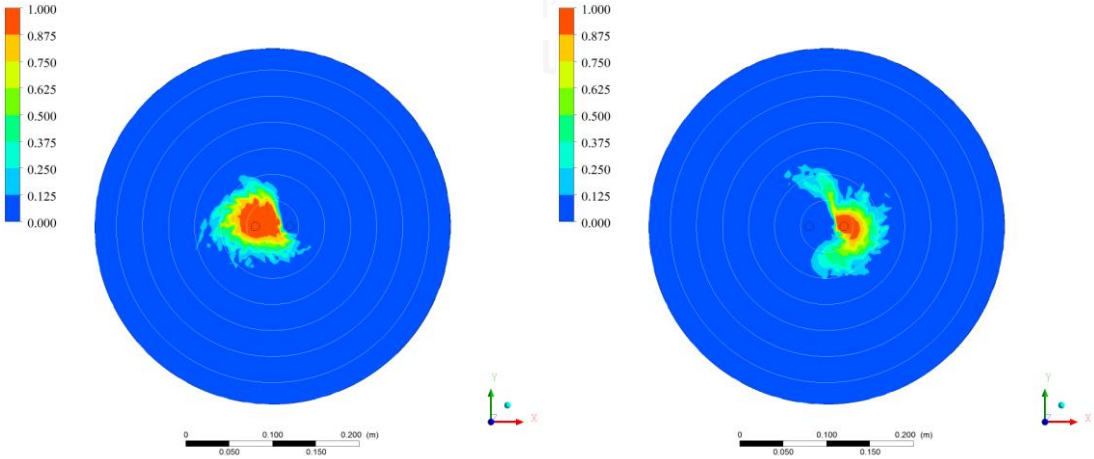

(c) 400 μm from disc

Figure 4.22 Cross-sectional volume fraction contours of water (LHS) and n-heptane (RHS) at 100, 200 and 400 μm with disc rotating speed of 250 rpm and both liquid flow rate of 15.708 mL/s each

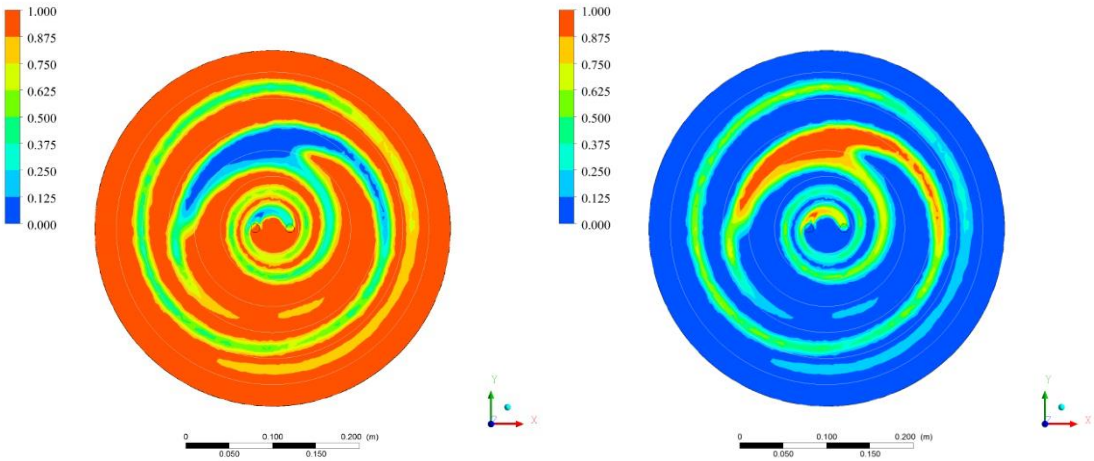

(a) at disc surface

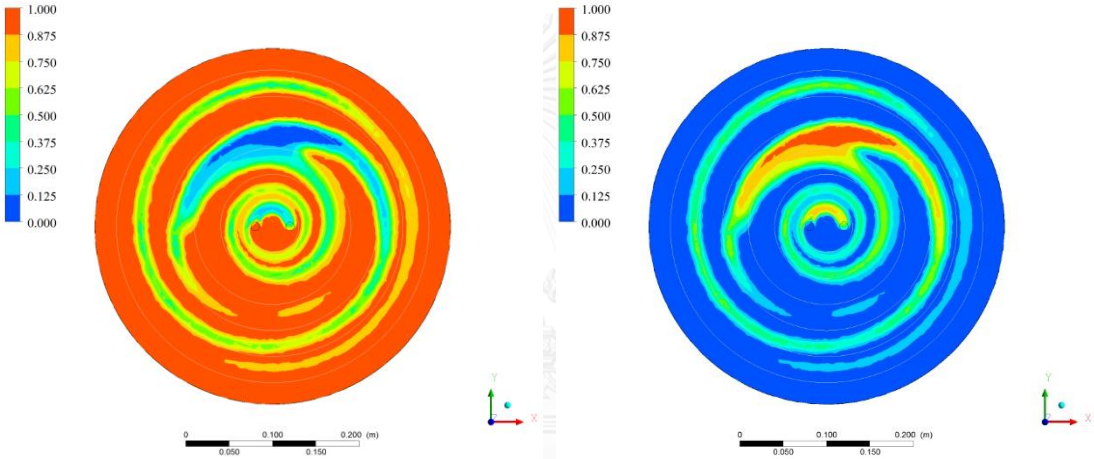

(b) 10 μm from disc

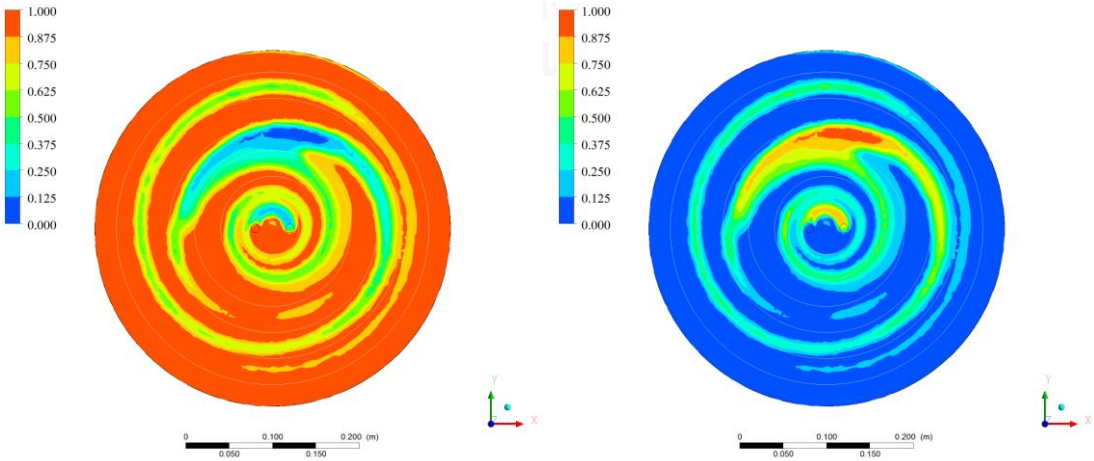

(c) 20 μm from disc

Figure 4.23 Cross-sectional volume fraction contours of water (LHS) and n-heptane (RHS) at disc surface, 10 and 20 μm with disc rotating speed of 50 rpm and both liquid flow rate of 15.708 mL/s each

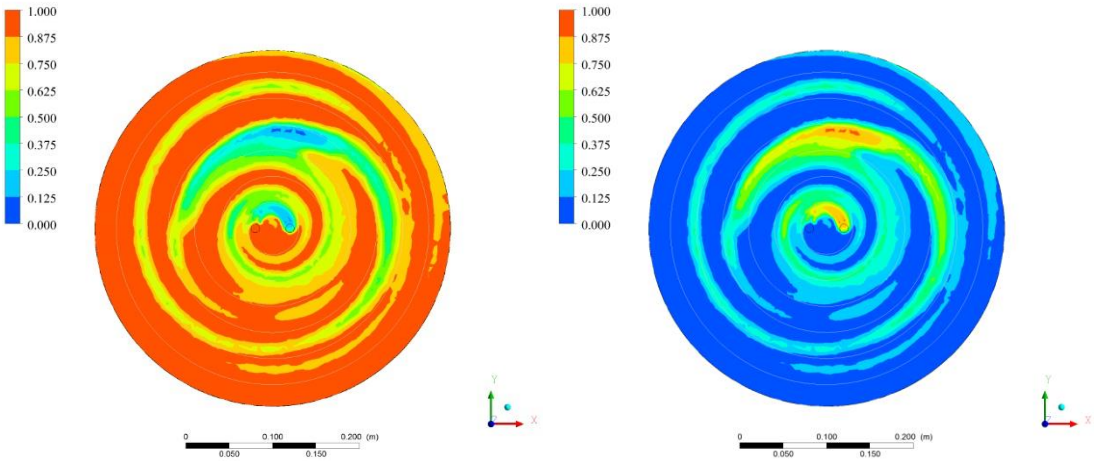

(a) 30 μm from disc

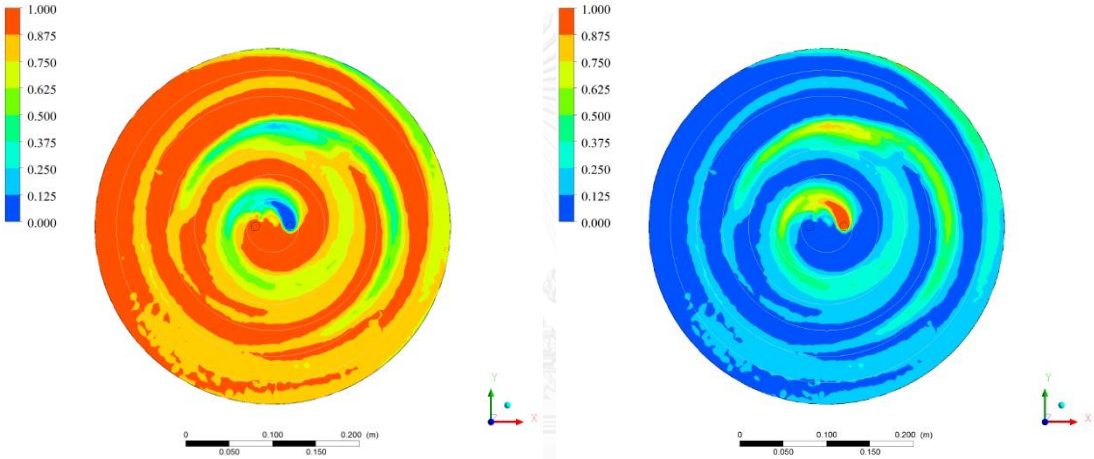

(b) 50 μm from disc

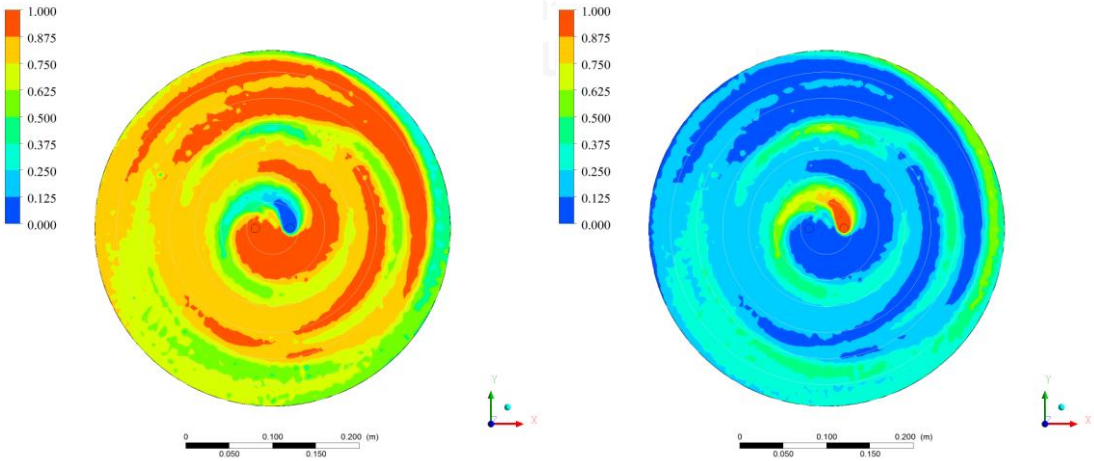

(c) 75 μm from disc

Figure 4.24 Cross-sectional volume fraction contours of water (LHS) and n-heptane (RHS) at 30, 50 and 75 μm with disc rotating speed of 50 rpm and both liquid flow rate of 15.708 mL/s each

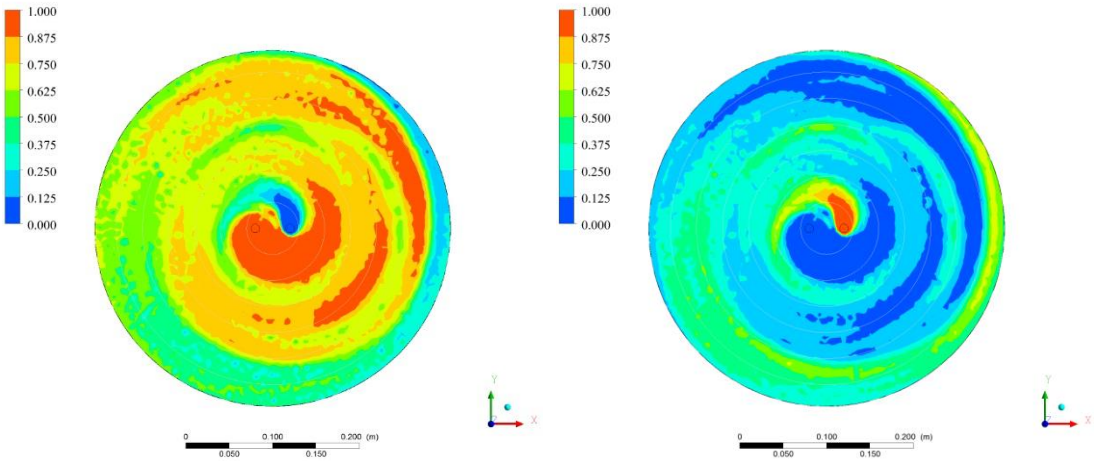

(a) 100 μm from disc

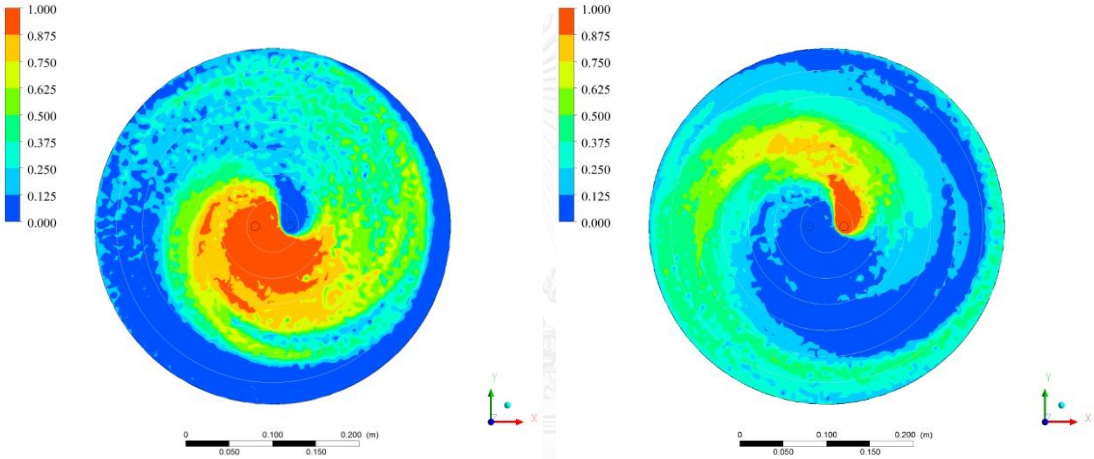

(b) 200 μm from disc

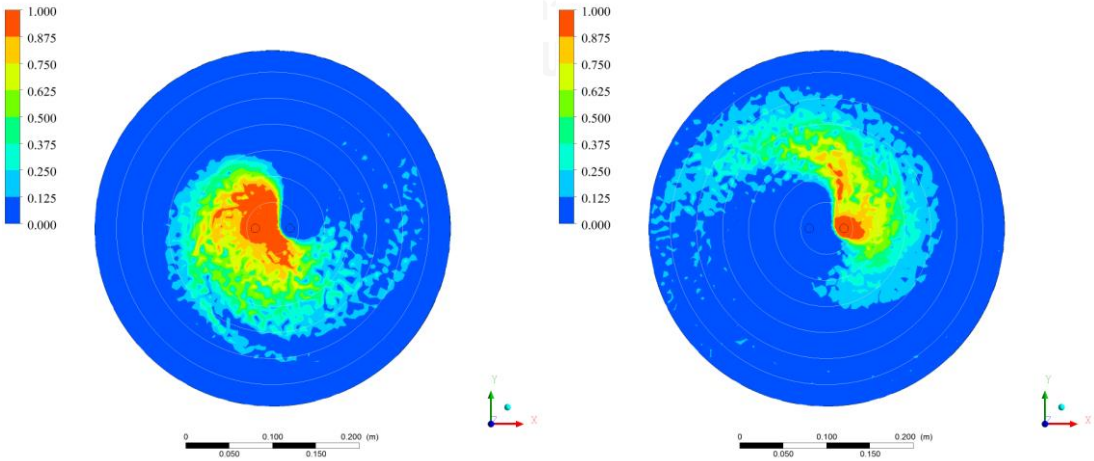

(c) 400 μm from disc

Figure 4.25 Cross-sectional volume fraction contours of water (LHS) and n-heptane (RHS) at 100, 200 and 400 μm with disc rotating speed of 50 rpm and both liquid flow rate of 15.708 mL/s each

Besides, in the very high speed range, the computed solutions at the rotating speeds of 500 and 1000 rpm are converged, except 1000 rpm case at the flow rate of 15.708 mL/s which will be discussed later. Nevertheless, the mixed liquid film is found to have some pits, the region on the rotating disc that liquid film does not exist, which means the disc is not totally covered by mixed liquid film. Consequently, operating in this condition may cause a problem, especially applications or processes which require liquid film uniformity e.g. nanoparticles production. Also, the performance of SDR will be difficult to predict because of these film defects. By the reasons above, the cases with film defects are not determined.

4.3 EFFECTS OF ADDITIONAL DESIGN PARAMETERS

Study of operational parameters, rotating speed and amount of liquid flow rate, to the performance of the SDR, interfacial area and mean residence time of each liquids, has early done. Henceforth, a constraint from amount of input materials and adaptation of liquid feedings are going to be studied for the sake of future SDR designs. Then, as the reference, the early case of 175 rpm with each liquid flow rate of 15.708 mL/s is chosen to be default. This reference case operates with highest flow rate, which gives high interfacial area and low residence time, and intermediate rotating speed, to avoid instability from operating at extreme speed. Moreover, the film uniformity is in the satisfied level.

4.3.1 Ratio of input immiscible liquids

Actually, each of chemical reactions or processes has a unique proportion of reactants or materials consumption, which is a design condition or a constraint for SDR design or operation. Thus, the flows of water and n-heptane are adjusted unequally to observe their effects to the interfacial area and residence times of both liquids.

All cases are fixed a total input flow rate of both liquids to 31.416 mL/s. The volumetric flow rates of each liquids are formerly equal at 15.703 mL/s each. Both liquid flow rates are adjusted to other values, but the total flow rate is kept constant at 31.416 mL/s. The ratio of water flow rate to n-heptane is changed to 3:1 and 1:3. The results of interfacial area and mean residence time are demonstrated in Table 4.2 and 4.3 respectively.

Table 4.2 Interfacial area between water and n-heptane with the change of flow rate ratio

Flow rate [mL/s]		Ratio of water to n-heptane	Interfacial area [m^2]	
water	n-heptane		amount	% change
15.708	15.708	1:1	0.0309138	
23.562	7.854	3:1	0.00428529	-86.14
7.854	23.562	1:3	0.110157	256.34

Table 4.3 Mean residence time of water and n-heptane with the change of flow rate ratio

Flow rate [mL/s]		Ratio of water to n-heptane	Mean residence time [s]			
water	n-heptane		water		n-heptane	
			amount	% change	amount	% change
15.708	15.708	1:1	0.844		0.607	
23.562	7.854	3:1	0.736	-12.73	0.627	3.32
7.854	23.562	1:3	0.993	17.73	0.613	0.93

As the flow rate of water is more than n-heptane at the ratio of 3:1, the interfacial area is deeply less than the reference case 86.14%, decreasing from 3.09×10^{-2} to 4.29×10^{-3} m^2. However, the interfacial area vividly increases approximately 2.5 times from the reference value to 1.10×10^{-1} m^2 when the n-heptane flow rate is three times of the water, vice versa. Remember that both liquids enter the reactor at a symmetric distance of 2 cm from the disc center. Thereby, the difference of physical properties between water and n-heptane may be significant to this strong change of interfacial area from varying the flow rate ratio.

As for the mean residence time, the higher proportion of water reduces itself residence time but raise the time of n-heptane. However, the rise of n-heptane flow rate over water causes the residence time of water longer but the change of n-heptane residence time is insignificant. Therefore, the response of mean residence time to the change of flow rate ratio cannot be predicted here.

4.3.2 Shifting of liquid feeding positions

Since there is no regulations of inlet positioning, the effect of inlet shifting distance from center is concerned. Although the variations of inlet feeding arrangement are unlimited, the inlets are shifted only in radial direction and along a same row with the disc center by preliminary. As shown in Figure 4.26, the shifting distances of water and n-heptane, R_w and R_h respectively, do not have to be equivalent, but the feeding height from rotating disc surface must be remained at 3 mm as it was.

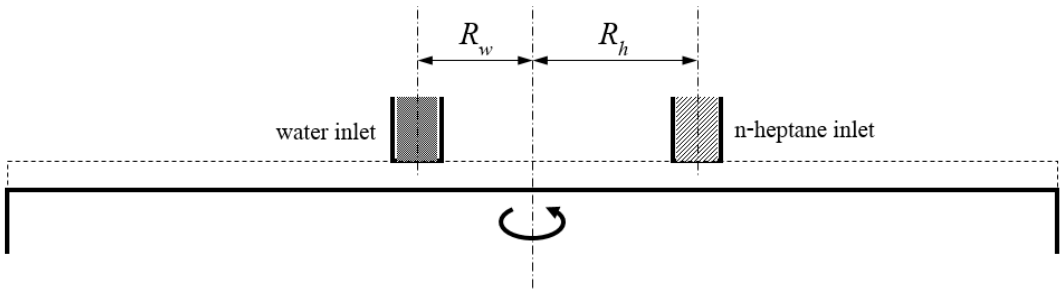

Figure 4.26 Shifting of liquid feeding positions from the disc center

The inlets of both liquids are shifted to various distances. The computed results are listed in Table 4.4 and compared with the original case, which inlets equally shifted from the center 2 cm each. Then, shifting of water inlet to the radius of 4 and 6 cm, while the n-heptane remains at 2 cm, is obtained to increase the interfacial area 30.49% and 34.53% respectively from the original. However, the area decreases 66.25% and 75.65% in case of the water inlet stays at the default position of 2 cm but the n-heptane inlet is shifted to 4 and 6 cm. According to these changes, a prediction of the interfacial area provided from asymmetric position change of both inlets cannot be conclude. Somehow, further shifting both inlets symmetrically, 4, 6 and 8 cm each, from the center definitely decreases the interfacial area.

Table 4.4 Interfacial area and mean residence time of water and n-heptane with the various shifting liquid inlet position from the disc center

Shifted distance [cm]		Interfacial area [m^2]		Mean residence time (s)			
				water		n-heptane	
R_w	R_h	amount	% change	amount	% change	amount	% change
2	2	0.0309138		0.844		0.607	
4	2	0.0403391	30.49	0.743	-11.98	0.716	17.97
6	2	0.0415874	34.53	0.613	-27.31	0.824	35.73
2	4	0.0104324	-66.25	0.936	11.04	0.543	-10.66
2	6	0.0075270	-75.65	0.990	17.35	0.491	-19.09
4	4	0.0288997	-6.52	0.841	-0.33	0.610	0.52
6	6	0.0190475	-38.39	0.808	-4.23	0.596	-1.91
8	8	0.0064436	-79.16	0.770	-8.72	0.513	-15.53

In terms of mean residence time, either liquid which of inlet shifted out asymmetrically has a reduced residence time, whereas another liquid which remains the default position gains more residence time. Nevertheless, if both feedings are shifted by equal distance, the mean residence times decrease proportionally except for n-

heptane in the case of 4 cm each. The mean residence time of n-heptane increases for 0.52% but it is practically insignificant.

4.3.3 Number of liquid feedings and liquid inlet arrangement

Moreover, designs of SDR with more inlets are interesting. Then, in this work, two more liquid inlets are tentatively added above the rotating disc to be four inlets. All inlets are symmetrically placed far from the disc center 2 cm. Each inlets are assigned to discharge one immiscible liquid. The liquid inlet arrangements are demonstrated in Figure 4.27, while the W sign stands for water and H for n-heptane.

(a) normal 2 inlets *(b) 4 inlets, type I* *(c) 4 inlets, type II*

Figure 4.27 Arrangements of liquid inlets

The total liquid inlet flow rate is controlled at 31.416 mL/s. The amount of volumetric flow rate is divided equally by the number of inlets. Which case has two inlets, each of them release the flow rate of 15.708 mL/s. Likewise, for four inlets case, the flow rate is 7.854 mL/s each. The results are shown in Table 4.5.

Table 4.5 Interfacial area and mean residence time of water and n-heptane with two or four liquid inlets and different arrangements

Inlet arrangement	Interfacial area [m^2]		Mean residence time (s)			
			water		n-heptane	
	amount	% change	amount	% change	amount	% change
2 inlets	0.0309138		0.844		0.607	
4 inlets, type I	0.0113079	-63.42	0.938	11.15	0.620	2.05
4 inlets, type II	0.0171092	-44.65	0.937	11.06	0.597	-1.62

As if the augmentation of inlets is not helpful, all two cases with four inlets have the less interfacial area than the default case with two inlets. Furthermore, the mean residence times of water of both four inlets cases increase by 11% whereas the residence time change of n-heptane is meaningless.

4.4 MIXING LIQUID FILM DYNAMICS

In this section, the fluid dynamic aspect of mixing liquids film flow on the rotating disc will be discussed. Samples of film dynamics are collect from the SDR operating at 175 rpm with the flow rate of each liquids of 15.708 mL/s, along the dotted line from the center to the right edge as shown in Figure 4.28.

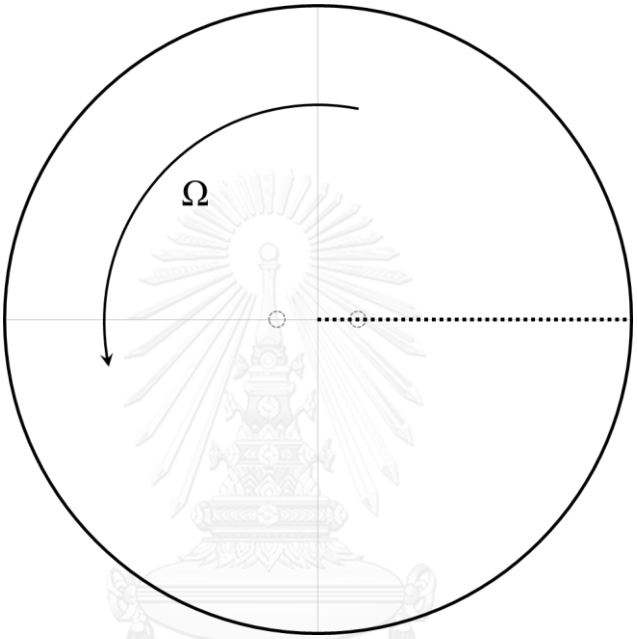

Figure 4.28 Position of the film dynamics samples (dotted line)

First, for the description of film dynamics, a film thickness profile is often used. The thickness profile of film along the sample line is illustrated in Figure 4.29. The velocity profile of liquid film system is normally compared or non-dimensionalized with the film height. Then, tangential and radial velocity profiles are collected from many radii along the sample line. All collected profiles are normalized with the disc tangential velocity, and also axial distance with the film thickness.

The velocities in tangential component are shown in Figure 4.30. The magnitudes of tangential velocity adjacent to disc surface are equal to disc speed. At the higher point within the film, deficit of tangential velocity appears. This occurrence is very clear at the radius of 3 cm, the tangential velocity is near zero at the film surface. However, as the radius of position increases, the deficit of velocity is less significant

when compared to the magnitude of disc speed. Therefore, the tangential velocity at the outer radius can be assumed uniform within liquid film.

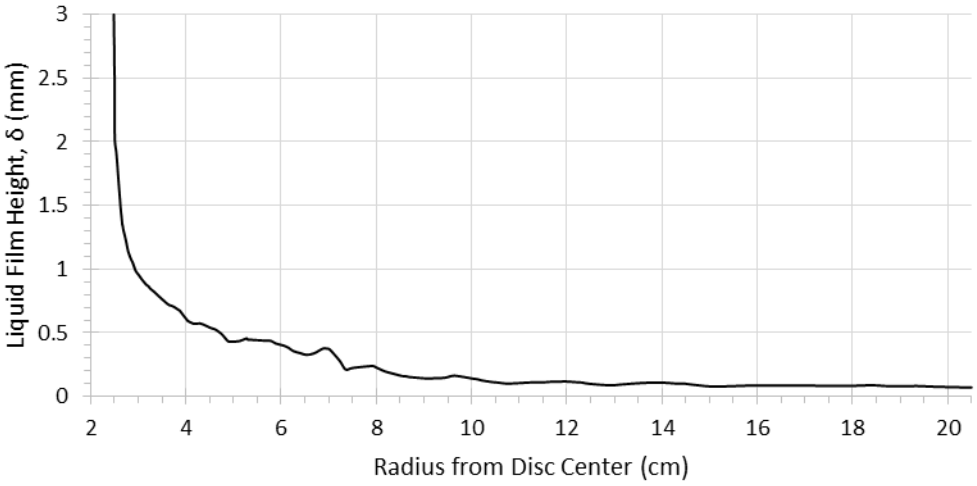

Figure 4.29 Liquid film height along the sample line

For radial components of velocity, they are also compared with the disc speed magnitude, Figure 4.31. All radial velocities of mixing liquid at the disc surface are zero on account of no-slip condition. At 3 cm, the radial profile is found to have the maximum and then decreases from that point beyond to the film surface. The role of radial components gradually dwindles at the outer radius when compared to the disc speed, but still exists for driving liquid film to the edge.

In addition, some former researches about SDR have mentioned the terms ‘centrifugal force’ and ‘Coriolis force’, which are used for description in non-inertial rotating frame of reference. Thus, it seems interesting if the flow inside SDR in this work can be describe with these regimes. In general, an absolute acceleration can be distributed to five terms in a rotating reference frame, written as

$$\vec{a} = \frac{d^2\vec{r}_o}{dt^2} + \frac{d\vec{\Omega}}{dt} \times \vec{r} + \vec{\Omega} \times \left(\vec{\Omega} \times \vec{r}\right) + \frac{d\vec{V}}{dt} + 2\vec{\Omega} \times \vec{V} \tag{4.6}$$

The spinning disc observed from a rotating frame, which of an origin attached to the disc axis of rotation and rotates with the same constant speed of disc, has no motion. Then, if the flow is observed from this rotating frame, the first and second terms of the right hand side of Eq. 4.6 are vanished and the conservation of momentum equation in the rotating frame is stated by

$$\rho\vec{a} = \rho\left(\frac{d\vec{V}}{dt} + \vec{\Omega}\times\left(\vec{\Omega}\times\vec{r}\right) + 2\vec{\Omega}\times\vec{V}\right) = -\nabla p + \nabla\cdot[\mu(\nabla\vec{u} + (\nabla\vec{u})^T)] + \rho\vec{g} \quad (4.7)$$

which can be rewritten as

$$\rho\frac{d\vec{V}}{dt} = \vec{f} - \left[\rho\vec{\Omega}\times\left(\vec{\Omega}\times\vec{r}\right)\right] - \left[2\rho\vec{\Omega}\times\vec{V}\right] \quad (4.8)$$

where

$$\vec{f} = -\nabla p + \nabla\cdot[\mu(\nabla\vec{u} + (\nabla\vec{u})^T)] + \rho\vec{g}$$

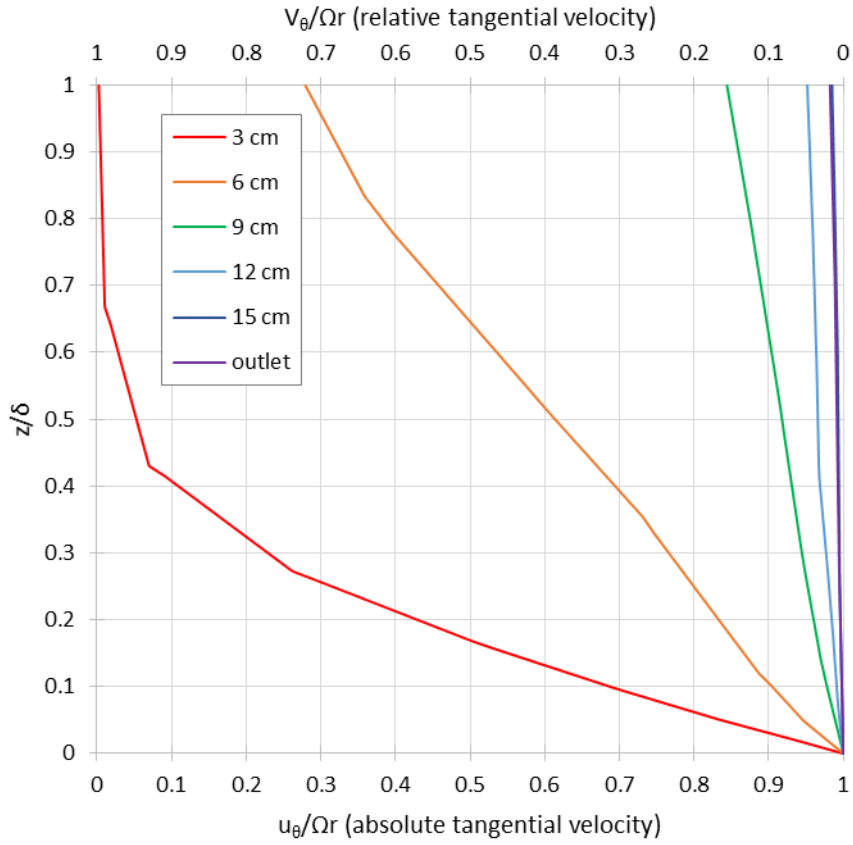

Figure 4.30 Non-dimensional tangential velocity profiles

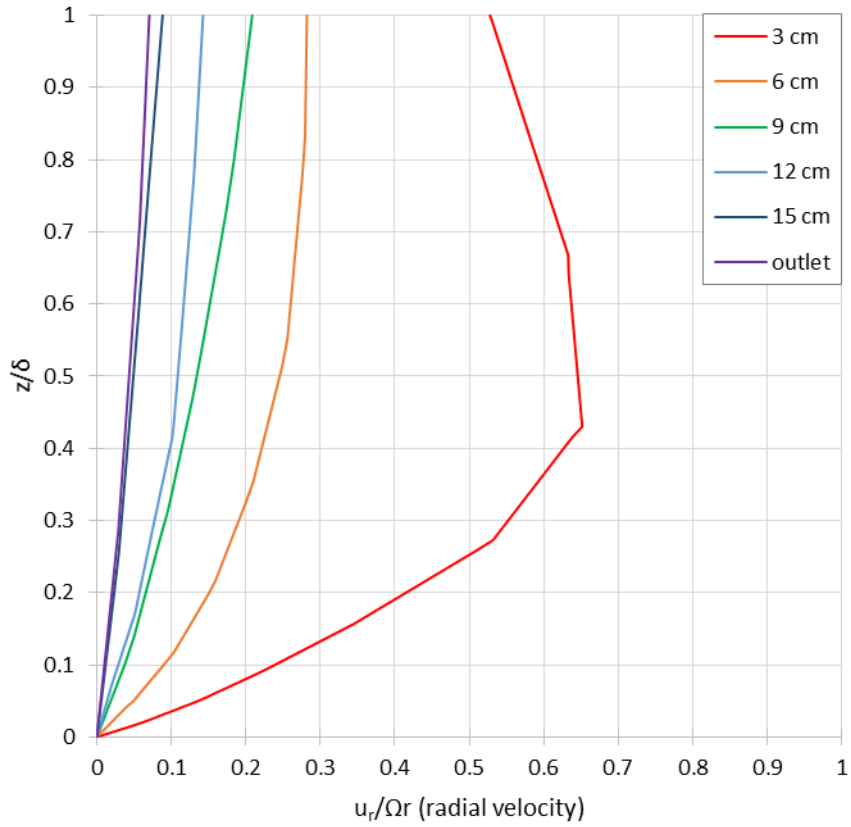

Figure 4.31 Non-dimensional radial velocity profiles

When the system is observed with the rotating frame, apart from pressure force, shear force and gravitational body force, there are two additional terms which affect the flow. These are called 'fictitious forces', the forces that appear when observed by the rotating frame. The second and third terms of the right hand side of Eq. 4.8 are centrifugal force and Coriolis force, respectively. Forasmuch the centrifugal force directs outward the disc center radially and depends on the radial distance from the rotating frame origin, this force can only affect the radial component of velocity.

4.5 APPLICATIONS OF THE RESULTS FROM THIS STUDY

All the results have to be analyzed for synthesizing the fundamentals for applications. Any processes have its own favorable operating condition to increase SDR efficiency. The first thing that have to be concerned is, the rotating speed and the amount of input liquid flow rate must be synchronized. Moreover, the rotating speed must be adjusted within the appropriate range. Lack of speed may cause hydraulic jump

on the disc, which is unfavorable instability of film. Too much speed causes defects on the mixing liquid film. These two problems can create trouble in nanoparticle production and other processes which need liquid film uniformity.

Operating an SDR within the low speed range seems to gain more interfacial area between immiscible liquids. Nevertheless, remember that, less the rotating speed, more residence time of the materials inside and more getting close to the instability. Thus, there is another choice for increasing interfacial area and also decreasing residence time, by increases the flow rates of liquid. If the process mainly have to lean on mixing without other constraints, try to operate with more liquid flow and low rotating speed as possible. However, if process needs uniformity of liquid film, there is no choices and the rotating speed must be set to high. For increasing the interfacial area, only the liquid flow rate can be increased.

In design aspect, adding more inlets and place at the same distance next to the center is useless, even shifting inlets equally also. These all strongly decreases the interfacial area of two liquids which is the core of this work. However, shifting liquid feeding at asymmetric positions has more potential to improve the performance of SDR.

Finally, if the process has a constraint on the ratio of reactants or materials and provides unsatisfied performance, try to modulate the rotating speed and the total flow rate likewise, or design an SDR to have adjustable inlet positions and place inlets at the asymmetric position.

CHAPTER 5
CONCLUSION

The spinning disc reactor with two inlets above the disc was simulated in this research, to observe its performance. All the results and recommendations are summarized in this chapter.

5.1 SUMMARY OF RESULTS

Two performances studied in this work are the interfacial area and the mean residence time. A high value of the interfacial area implies better mixing and enhancement of mass transfer rate or chemical reaction rate, if exists. Disc rotating speeds and liquid flow rates are main operative parameters which affect the SDR performance. Increasing the speed of disc reduces mean residence time of liquids and maintain the mixing liquid film uniformity, but also decreases the interfacial area. However, the interfacial area can be gained by increasing liquid flow rate. Increasing of liquid flow rate also reduces residence time of liquid, but instability of film can occur. The reactor must be operated in the appropriate range of rotating speed. Extremely low speeds can cause hydraulic jump and very high speeds cause film defects.

After the operative parameters are revealed their effects, a constraint of flow rate ratio and inlet positions are studied. Flow rate ratio of two liquids strongly affects the interfacial area. If the flow rate of lower dense liquid increases, the mixing liquids gain more interfacial area. However, the mean residence time change with flow rate ratio cannot be concluded. Next, the inlet positions are shifted further more from the center, but result in worse performance, the interfacial area decreases. Nevertheless, only shifting water inlet further away from the center, with n-heptane position remains the same, increases the interfacial area. Moreover, adding more inlets is not a good choice to improve the reactor performance, since the interfacial area decreases without any advantages from residence time

5.2 RECOMMENDATIONS

Finally, the ways for improving the spinning disc reactor performance are now widely open. The effects from stationary casing, roughness of the disc and more configuration of feeding inlets are worth finding. More operation constraints should be taken into account and analyzed for the sake of appropriate design.

REFERENCES

1. Chen, K.-J. and Y.-S. Chen, *Intensified production of biodiesel using a spinning disk reactor.* Chemical Engineering and Processing: Process Intensification, 2014. **78**: p. 67-72.
2. Visscher, F., et al., *Liquid–liquid mass transfer in a rotor–stator spinning disc reactor.* Chemical Engineering Journal, 2012. **185-186**: p. 267-273.
3. De Caprariis, B., et al., *CFD Model of a Spinning Disk Reactor for Nanoparticle Production.* Chemical Engineering Transactions 2015. **43**: p. 757-762.
4. Akhtar, M., B.S. Murray, and S. Dowu, *A novel continuous process for making mayonnaise and salad cream using the spinning disc reactor: Effect of heat treatment.* Food Hydrocolloids, 2014. **42**: p. 223-228.
5. Gakis, G.P., E.D. Koronaki, and A.G. Boudouvis, *Numerical investigation of multiple stationary and time-periodic flow regimes in vertical rotating disc CVD reactors.* Journal of Crystal Growth, 2015. **432**: p. 152-159.
6. Peshev, D., G. Peev, and A. Nikolova, *Dissolution in film flow of shear thinning liquid on a horizontal rotating disk.* Chemical Engineering and Processing: Process Intensification, 2010. **49**(6): p. 616-621.
7. Vicevic, M., K.V.K. Boodhoo, and K. Scott, *Catalytic isomerisation of α-pinene oxide to campholenic aldehyde using silica-supported zinc triflate catalysts.* Chemical Engineering Journal, 2007. **133**(1-3): p. 43-57.
8. Hirt, C.W. and B.D. Nichols, *Volume of fluid (VOF) method for the dynamics of free boundaries.* Journal of Computational Physics, 1981. **39**: p. 201-225.
9. Leonard, B.P., *A Stable and Accurate Convective Modelling Procedure Bassed on Quadratic Upstream Interpolation.* Comput. Methods Appl. Mech. Eng., 1979. **19**: p. 59-98.
10. Versteeg, H.K. and W. Malalasekera, *An Introduction to Computational Fluid Dynamics: The Finite Volume Method.* 2007.
11. *ANSYS FLUENT Theory Guide*. 2013: ANSYS Inc.
12. Patankar, S.V., *Numerical Heat Transfer and Fluid Flow.* 1980.
13. Ong, C.L. and J.M. Owen, *Computation of the flow and heat transfer due to a rotating disc.* International Journal of Heat and Fluid Flow, 1991. **12**(2): p. 106-115.
14. Theodorsen, T. and A. Regier, *Experiments on drag of revolving disks, culinders, and streamline rods at high speeds.* NACA Rep., 1944. **793**.
15. Leshev, I. and G. Peev, *Film flow on a horizontal rotating disk.* Chemical Engineering and Processing: Process Intensification, 2003. **42**(11): p. 925-929.
16. Lepehin, G.I. and G.V. Riabchuk, *Temperature distribution in film of viscous liquid with heating on a rotating disk.* Rheology in Processes and Apparatus of Chemical Technology, 1975: p. 82–91.
17. Rauscher, J.W., R.E. Kelly, and J.D. Cole, *An Asymptotic Solution for the Laminar Flow of a Thin Film on a Rotating Disk.* Journal of Applied Mechanics, 1973. **40**(1): p. 43-47.

VITA

Mister Pichaya Sompopskul was born in Nonthaburi, Thailand. Studied at Saint Gabriel's College in high school level. Graduated from Chulalongkorn University, Bangkok, Thailand, in Bachelor's Degree of Mechanical Engineering.